

Epac1 mediates protein kinase A-independent mechanism of forskolin-activated intestinal chloride secretion

Kazi Mirajul Hoque,¹ Owen M. Woodward,² Damian B. van Rossum,³ Nicholas C. Zachos,¹ Linxi Chen,¹ George P.H. Leung,⁴ William B. Guggino,² Sandra E. Guggino,^{1,2} and Chung-Ming Tse¹

¹Department of Medicine, GI Division, ²Department of Physiology, and ³Department of Neuroscience, Johns Hopkins University, Baltimore, MD 21205

⁴Department of Pharmacology, The University of Hong Kong, Hong Kong, China

Intestinal Cl^- secretion is stimulated by cyclic AMP (cAMP) and intracellular calcium ($[\text{Ca}^{2+}]_i$). Recent studies show that protein kinase A (PKA) and the exchange protein directly activated by cAMP (Epac) are downstream targets of cAMP. Therefore, we tested whether both PKA and Epac are involved in forskolin (FSK)/cAMP-stimulated Cl^- secretion. Human intestinal T84 cells and mouse small intestine were used for short circuit current (I_{sc}) measurement in response to agonist-stimulated Cl^- secretion. FSK-stimulated Cl^- secretion was completely inhibited by the additive effects of the PKA inhibitor, H89 (1 μM), and the $[\text{Ca}^{2+}]_i$ chelator, 1,2-bis-(o-aminophenoxy)-ethane-*N,N,N',N'*-tetraacetic acid, tetraacetoxymethyl ester (BAPTA-AM; 25 μM). Both FSK and the Epac activator 8-pCPT-2'-O-Me-cAMP (50 μM) elevated $[\text{Ca}^{2+}]_i$, activated Ras-related protein 2, and induced Cl^- secretion in intact or basolateral membrane-permeabilized T84 cells and mouse ileal sheets. The effects of 8-pCPT-2'-O-Me-cAMP were completely abolished by BAPTA-AM, but not by H89. In contrast, T84 cells with silenced Epac1 had a reduced I_{sc} response to FSK, and this response was completely inhibited by H89, but not by the phospholipase C inhibitor U73122 or BAPTA-AM. The stimulatory effect of 8-pCPT-2'-O-Me-cAMP on Cl^- secretion was not abolished by cystic fibrosis transmembrane conductance (CFTR) inhibitor 172 or glibenclamide, suggesting that CFTR channels are not involved. This was confirmed by lack of effect of 8-pCPT-2'-O-Me-cAMP on whole cell patch clamp recordings of CFTR currents in Chinese hamster ovary cells transiently expressing the human CFTR channel. Furthermore, biophysical characterization of the Epac1-dependent Cl^- conductance of T84 cells mounted in Ussing chambers suggested that this conductance was hyperpolarization activated, inwardly rectifying, and displayed a $\text{Cl}^- > \text{Br}^- > \text{I}^-$ permeability sequence. These results led us to conclude that the Epac-Rap-PLC- $[\text{Ca}^{2+}]_i$ signaling pathway is involved in cAMP-stimulated Cl^- secretion, which is carried by a novel, previously undescribed Cl^- channel.

INTRODUCTION

The CFTR is the major Cl^- channel found in the apical membrane of intestinal and airway epithelial cells. PKA phosphorylates and opens CFTR (Barrett, 2000; Barrett and Keely, 2000; Huang et al., 2000). Therefore, most studies on intestinal and airway Cl^- secretion have focused on PKA as the downstream target of cAMP. Two major intracellular cAMP receptors are now known to mediate cAMP effects in vivo: the classical cAMP-dependent PKA pathway and the recently discovered exchange

protein directly activated by cAMP (Epac). Epac, upon binding of cAMP, activates PKA-independent signaling cascades via small G proteins (de Rooij et al., 1998; Kawasaki et al., 1998). Many cAMP-mediated physiological processes that were previously thought to be solely mediated by PKA have now been shown to be mediated in parallel by Epac (Bos, 2006). For instance, glucagon-like peptide 1 is a cAMP-elevating agent. It stimulates insulin secretion in pancreatic β cells via both PKA- and Epac-dependent pathways, and the latter involves Ca^{2+} -dependent exocytosis of insulin granules and inhibition of ATP-sensitive K^+ channels (K_{ATP} channels) (Holz, 2004; Kang et al., 2008).

Human intestinal T84 cells have been used as a model for studying the physiology and regulation of intestinal Cl^- secretion (Dharmasathaphorn and Madara, 1990). The

Correspondence to Chung-Ming Tse: mtse@jhmi.edu; or Kazi Mirajul Hoque: kmh_niced@yahoo.co.in

Abbreviations used in this paper: BAPTA-AM, 1,2-bis-(o-aminophenoxy)-ethane-*N,N,N',N'*-tetraacetic acid, tetraacetoxymethyl ester; $[\text{Ca}^{2+}]_i$, intracellular calcium; CaCC, calcium-activated Cl^- channel; CFTRinh-172, CFTR inhibitor 172; CHO, Chinese hamster ovary; CLC2, Cl^- channel isoform 2; DIDS, 4,4'-diisothiocyanatostilbene-2,2'-disulphonic acid; Epac, exchange protein directly activated by cAMP; FSK, forskolin; I_{Cl} , chloride conductance; I_{sc} , short circuit current; LaCl_3 , lanthanum chloride; NPPB, 5-nitro-2-(3-phenylpropylamino)-benzoate; Rap2, Ras-related protein 2; RT, reverse transcription; shRNA, short hairpin RNA; TRC, the RNA interference consortium; VIP, vasoactive intestinal peptide.

© 2010 Hoque et al. This article is distributed under the terms of an Attribution-Noncommercial-Share Alike-No Mirror Sites license for the first six months after the publication date (see <http://www.jgp.org/misc/terms.shtml>). After six months it is available under a Creative Commons License (Attribution-Noncommercial-Share Alike 3.0 Unported license, as described at <http://creativecommons.org/licenses/by-nc-sa/3.0/>).

current model of Cl^- secretion involves electroneutral Cl^- entry across the basolateral membrane via the $\text{Na}^+/\text{K}^+/\text{2Cl}^-$ cotransporter, followed by electrogenic Cl^- exit across the apical membrane via Cl^- channels. Simultaneous activation of basolateral K^+ channels maintains a favorable electrical gradient for apical Cl^- efflux by limiting cell depolarization. Because Cl^- carries a negative charge, the positively charged Na^+ ion follows the negative charge gradient across the epithelial cell layer through cation-selective tight junctions. Water, which is driven by the osmotic gradient, follows the net transepithelial NaCl movement (Barrett, 2000; Fuller and Benos, 2000).

Cyclic nucleotides such as cAMP are major regulators of Cl^- secretion in T84 cells. Forskolin (FSK), which acts on adenylate cyclase to elevate intracellular cAMP, and the cAMP analogue 8-Br-cAMP are commonly used to probe the mechanism of PKA-dependent stimulation of Cl^- secretion. However, it appears that PKA may not be the only target of cAMP because intracellular calcium ($[\text{Ca}^{2+}]_i$) can be elevated in response to FSK and/or cAMP. For instance, Merlin et al. (1998) previously showed that FSK elevates $[\text{Ca}^{2+}]_i$ by unknown mechanisms in T84 cells. Similarly, FSK/cAMP increases $[\text{Ca}^{2+}]_i$ in chicken enterocytes (Semrad and Chang, 1987). These observations suggest that FSK elicits Cl^- secretion by activating not only PKA, but also other signaling pathways such as $[\text{Ca}^{2+}]_i$. Furthermore, Epac has been shown to transduce cAMP into $[\text{Ca}^{2+}]_i$ signaling via PLC ϵ , and this effect of Epac is PKA independent (Schmidt et al., 2001). Because cAMP and $[\text{Ca}^{2+}]_i$ are major regulators of intestinal Cl^- secretion, we ask whether Epac plays a role in FSK- or cAMP-stimulated Cl^- secretion in intestinal epithelial cells, and whether Epac links intracellular cAMP signaling to $[\text{Ca}^{2+}]_i$ elevation, thus allowing cAMP to mediate Cl^- secretion in a PKA-dependent and -independent manner. Furthermore, Cl^- channels are a functionally and structurally diverse group, and some are involved in normal fluid transport across various epithelia (Kidd and Thorn, 2000; Hartzell et al., 2005; Verkman and Galletta, 2009). The CFTR channel is inhibited by CFTR inhibitor 172 (CFTRinh-172), and only the CFTR channel has been implicated in cAMP-activated Cl^- secretion in a variety of epithelia, including the airway and intestine (Riordan, 1993). However, the Epac-activated Cl^- secretion in the intestine was resistant to CFTRinh-172, and thus the present study also characterizes this new Cl^- conductance biophysically as well as pharmacologically.

MATERIALS AND METHODS

Materials

Cell culture reagents, TRIZOL, Fura2-AM, and BCECF-AM were from Invitrogen. All other reagents were obtained from Sigma-Aldrich, except 8-pCPT-2'-O-Me-cAMP (BioLog Life Science

Institute), U73122 (Enzo Life Sciences, Inc.), G66976 and CFTRinh-172 (EMD), glibenclamide (Research Biochemicals, Inc.), and Epac1 and Epac2 antibodies (sc-28366 and sc-28326, respectively; Santa Cruz Biotechnology, Inc.).

Cell culture and Ussing chamber setup

T84 cells were grown as confluent monolayers in a 1:1 mixture of Dulbecco's modified Eagle's medium (DMEM) and Ham's F-12 medium supplemented with 40 $\mu\text{g}/\text{ml}$ penicillin, 90 $\mu\text{g}/\text{ml}$ streptomycin, and 10% fetal bovine serum. Only monolayers with resistances in the range of 1,500 to 3,000 $\Omega\cdot\text{cm}^2$ were used for experiments, and these were mounted between two halves of an Ussing chamber for short circuit current (I_{sc}) measurement, which was done at 37°C with both sides of the monolayer immersed in an oxygenated HCO_3^- -free solution containing (in mM) 140 NaCl, 5 KCl, 1 MgCl_2 , 2 CaCl_2 , 10 HEPES, and 10 glucose, pH 7.4. 5 ml of fluid in each half of the chamber was connected via KCl agar bridges to voltage and current electrodes and clamped at 0 mV using VCC MC6 multi-channel voltage-current clamp amplifier (Physiologic Instruments). T84 cells with a stable knockdown of Epac1 (T84Epac1KD) were grown on transwell inserts in DMEM plus Ham's F-12 media containing 10 $\mu\text{g}/\text{ml}$ puromycin in addition to 40 $\mu\text{g}/\text{ml}$ penicillin, 90 $\mu\text{g}/\text{ml}$ streptomycin, and 10% fetal bovine serum. These cells were also studied using the same solution mentioned above for Ussing chambers.

Calcium imaging

T84 cells were grown on glass coverslips. Cells were loaded with 2 μM Fura 2-AM in HEPES-buffered salt solution (HBSS; in mM: 135 NaCl, 1.2 MgCl_2 , 1.2 CaCl_2 , 10 HEPES, 5 KCl, and 10 glucose, pH 7.4) by incubating for 30–45 min in the dark at 37°C, followed by a 30-min de-esterification in HBSS containing 5 μM indomethacin at room temperature. Fura 2 fluorescence images were monitored at a 510-nm emission with alternating excitation at 340 and 380 nm as described previously (Merlin et al., 1998). Individual Fura-2-loaded T84 cells were selected and $[\text{Ca}^{2+}]_i$ values were calculated on a pixel-by-pixel basis for data processing using Origin software (OriginLab). For calibration of the Ca^{2+} indicator, a Fura-2 Ca^{2+} -imaging calibration kit with 0–10 mM CaEGTA (Invitrogen) was used according to the manufacturer's instructions. All measurements shown are representative of a minimum of three independent experiments with no fewer than 50 cells calculated in each study.

Reverse transcription (RT)-PCR

Total RNA was isolated from T84 cells by TRIZOL reagent (Invitrogen). cDNA was synthesized from total RNA using random hexamers and superscript II RT. 1 μl of the first-strand cDNA product was then used as template for PCR amplification with Taq DNA polymerase by 30 thermocycles of 94°C for 1 min, 54°C for 1 min, and 72°C for 1 min using oligonucleotides specific for Epac1 (sense: TTCCTCCAGAACTCTCAG; antisense: TCAGCTCATCGCTTCCTG; size of PCR product is 460 bp) and Epac2 (sense: CTCATTGAACCTCAGTTCC; antisense: AGTCATCTCCTTCATGCAGG; size of PCR product is 500 bp).

Western blot analysis

Wild-type T84 or Epac-depleted cells (Epac1KDT84) were grown to 100% confluency on transwell permeable supports (in 75-mm dishes; Corning). Cells were scraped in PBS and then homogenized by sonication in RIPA buffer plus protease inhibitor cocktail (1:100; Sigma-Aldrich) to obtain total cell lysates. Total lysates of mouse mucosal cells were prepared from scrapings of duodenum, jejunum, ileum, or colon as described previously (Hillesheim et al., 2007). Lysates were analyzed by Western blot using an Epac1 mouse monoclonal and Epac2 rabbit polyclonal antibody, secondary polyclonal goat anti-mouse immunoglobulin G conjugated

to Alexa Fluor 680 (Invitrogen), and secondary goat anti-rabbit immunoglobulin G conjugated to IRDye 800 (Rockland Immunochemicals, Inc.). The expression of CFTR was determined by antibody 5959, which is a rabbit anti-human CFTR R domain polyclonal antibody generated by us to the peptide IEEDSDEPL-ERRLSLVPDSEQGE. The glyceraldehyde-3-phosphate dehydrogenase antibody was obtained from USBiological. The fluorescence signal was analyzed by the Odyssey Infrared Imaging System (LI-COR Biosciences).

Immunocytochemistry

Confluent T84 cells grown on 25-mm tissue culture inserts (Thermo Fisher Scientific) were fixed on ice in 3% paraformaldehyde solution in PBS (EM grade; Electron Microscopy Sciences). Cells were washed in ice-cold PBS and quenched with 50 mM NH₄Cl in PBS for 15 min on ice. Nonspecific staining was blocked in PBS containing 1% BSA and 0.075% saponin for 30 min on ice. An anti-Epac 1 antibody (1:10) was then added for 1 h at room temperature, after which excess antibody was washed in 0.1% BSA in PBS with 0.075% saponin. The cells were then incubated with a goat anti-mouse secondary antibody conjugated to Alexa 568 for an additional hour. After extensive washing of excess secondary antibody, cells were incubated with Hoechst 33324 (Invitrogen) and mounted on microscope slides. Microscopy was performed using an LSM 510 (Carl Zeiss, Inc.).

Activation of Ras-related protein 2 (Rap2)

Activation of Rap2 was determined by the EZ-Detect Rap activation kit (Thermo Fisher Scientific) with slight modifications. In brief, T84 cells were incubated with or without FSK and 50 μ M 8-pCPT-2'-O-Me-cAMP for 20 min at 37°C. These cells were lysed with 25 mM Tris/HCl, pH 7.5, 150 mM NaCl, 5 mM MgCl₂, 1% NP-40, 1 mM DTT and 5% glycerol, 10 mM NaF, and 1 mM Na₃VO₄ in the presence of a protease inhibitor cocktail (Sigma-Aldrich). After centrifugation at 16,000 *g* at 4°C for 15 min to remove insoluble materials, the supernatants (700 μ g of protein) were incubated with 20 μ g of glutathione-S-transferase-tagged RalGDS-RBD (Ras-binding domain of the Ral guanine nucleotide dissociation stimulator) and an Immobilized Glutathione Disc (resin; SwellGel) for 1 h at 4°C. The affinity-purified activated Rap proteins (Rap-GTP) were eluted with 50 μ l SDS/PAGE sample buffer containing 5% 2-mercaptoethanol and analyzed by Western blotting with anti-Rap2 antibody.

RNA interference

Mission, the RNA interference Consortium (TRC) lentiviral short hairpin RNA (shRNA) constructs, which target against Epac1, were obtained from Sigma-Aldrich (TRCN0000047228, TRCN0000047230, and TRCN0000047231). Lentiviral particles were produced in HEK293T cells grown on 10-cm plates by co-transfecting cells with lipofectamine 2000 with 3 μ g pVSVG (vesicular stomatitis virus glycoprotein), 9 μ g pCMV Δ R8.9, and 12 μ g shRNA plasmids. This mixture of lipofectamine and plasmids was added to the cells and incubated for 16 h. Transfection medium was then removed and replaced with fresh culture medium. Viral particles were then collected in 7 ml of medium 48 h after transfection. Viral supernatant was centrifuged at 1,000 rpm for 5 min and stored in aliquots at -80°C. For lentiviral transduction, T84 cells were grown on 35-mm dishes to ~70% confluency. On the day of transduction, the culture medium was replaced with 2 ml of fresh medium containing 2 mg/ μ l hexadimethrine bromide (Sigma-Aldrich). 1 ml of lentiviral particles was added to and incubated with cells for 20 h. The lentiviral particles were then removed, and the cells were replaced with fresh culture medium. 48 h after transduction, positively transduced cells were selected with 10 μ g/ml of puromycin-containing medium. Empty vector-

transduced T84 cells were processed and selected with puromycin in a similar manner.

Measurement of I_{sc} in mouse ileal sheets

All of the experimental protocols performed in this study were approved by the Institutional Animal Care and Use Committee of Johns Hopkins University. Non-fasting male mice (~35 g) were anesthetized and sacrificed by inhalation of halothane. The distal ileum was removed and partially stripped of serosal muscle layers. The mucosa was mounted in a tissue slider (2.8 \times 11-mm aperture for mouse tissue; area, 0.30 cm²) and bathed at 37°C on both sides with an HCO₃⁻-free solution, which was continually circulated with a gas lift oxygenated with 100% O₂. After tissues were mounted, the change in I_{sc} was monitored in real time (Hoque et al., 2005).

Measurement of chloride conductance (I_{Cl}) in permeabilized T84 monolayers

The effects of FSK and 8-pCPT-2'-O-Me-cAMP on apical membrane I_{Cl} were assessed after permeabilization of the basolateral membrane with 50 μ g/ml nystatin and the establishment of a basolateral to apical Cl⁻ concentration gradient (Lewis et al., 1977; Mun et al., 1998). 35 μ M ouabain was added to the basolateral bath to inhibit the Na⁺-K⁺-ATPase (Huflejt et al., 1994). Both apical and basolateral baths were initially filled with a Cl⁻-free/high K⁺ solution containing 10 mM sodium gluconate, 140 mM potassium gluconate, 1 mM calcium gluconate, 10 mM glucose, and 10 mM HEPES, pH 7.4. After equilibration, the basolateral solution was replaced with a high Cl⁻/high K⁺ solution containing 10 mM NaCl, 140 mM KCl, 1 mM MgSO₄, 1 mM CaCl₂, 10 mM glucose, and 10 mM HEPES, pH 7.4. 50 μ g/ml nystatin was then added to permeabilize the basolateral membrane to potassium and chloride. Under these conditions, there was an agonist-induced I_{Cl} as Cl⁻ ions from the cell moved down the concentration gradient through the Cl⁻ channels in the apical membrane. To do a biophysical characterization of the Epac-stimulated Cl⁻ conductance in T84 cells, we measured the I-V relationship. To do this, the voltage across the monolayer was sequentially stepped from a holding voltage of 0 mV to values between -100 and +100 mV in 20-mV increments with a pulse duration of 5 s while the corresponding transepithelial currents were recorded. For the graphical representation of the I/V relationship, we did not use the customary Ussing convention for I_{sc} s, where the voltage is V2-V1, where V1 is basolateral and V2 is apical (apical-basolateral). Instead, we used the physiological convention of inside-outside, which, when the basolateral side has been permeabilized to Cl⁻, can also be thought of as basolateral-apical. Using the physiological convention allows for a comparison of the I/V obtained here to the I/V relation of other Cl⁻ conductances recorded using patch clamp methodology. A 50-s interval between each pulse was sufficient for recovery from activation. The protocol was performed as described above with basolateral membrane-permeabilized T84 cells and after sustained stimulation with FSK or 8-pCPT-2'-O-Me-cAMP. Finally, we investigated the selectivity of the FSK-activated, CFTR-inhibited Epac-mediated Cl⁻ currents by substituting high concentrations of either I⁻ (150 mM) or Br⁻ (150 mM) on the basolateral side to measure the resulting I_{sc} in permeabilized membranes. The nystatin permeability of Cl⁻, Br⁻, and I⁻ is based on their hydrated radius (Cass et al., 1970), which is nearly identical (3.32, 3.30, and 3.31 Å) (Conway, 1981). Therefore, we have assumed an equal nystatin permeability for our selectivity experiments. The relative permeability of Cl⁻, Br⁻, and I⁻ was calculated from the Goldman-Hodgkin-Katz equation. Various blockers of epithelial chloride channels such as Zn, Cd, 4,4'-diisothiocyanatostilbene-2,2'-disulphonic acid (DIDS), 5-nitro-2-(3-phenylpropylamino)-benzoate (NPPB), niflumic acid, glibenclamide, and GlyH-101 were used to further characterize this conductance.

Patch clamp recording

Whole cell recordings were performed in Chinese hamster ovary (CHO) cells transiently transfected with a plasmid containing human CFTR tagged with EGFP. Cells were visualized using an Eclipse Fluorescent inverted microscope (Nikon). Whole cell currents were input into an Axopatch 200B amplifier (Axon Instruments) and analyzed using PClamp 9.2 software (Axon Instruments). Cells were bathed in solution containing (in mM): 140 NaCl, 2 CaCl₂, 1 MgCl₂, 80 D-mannitol, and 10 HEPES, pH 7.4. The pipette solution consisted of (in mM): 135 CsCl, 2 MgCl₂, 2 ATP, 10 HEPES, and 0.001 free Ca²⁺, pH 7.4. The hypertonic bath solution was used to prevent the activation of any swelling activated Cl⁻ conductance.

Statistics

Results were analyzed by the statistic software Origin and presented as means \pm SE of at least three independent experiments. Comparisons between means were performed using Student's *t* tests. Differences among groups were determined using one-way ANOVA and Student-Newman-Keuls posttest. An overall *P* < 0.05 was considered significant.

Online supplemental material

The supplemental material includes the effect of lanthanum chloride (LaCl₃) and 2-APB on FSK-stimulated I_{sc} in T84 cells (Fig. S1) and the effect of U73122 and 1,2-bis-(*o*-aminophenoxy)-ethane-*N,N,N',N'*-tetraacetic acid, tetraacetoxymethyl ester (BAPTA-AM) on vasoactive intestinal peptide (VIP)-stimulated or 8-Br-cAMP-stimulated Cl⁻ secretion in T84 cells (Fig. S2). Fig. S3 shows that the Epac activator 8-pCPT-2'-O-Me-cAMP does not activate CFTR transiently expressed in CHO cells, which express endogenous Epac1. Figs. S1–S3 are available at <http://www.jgp.org/cgi/content/full/jgp.200910339/DC1>.

RESULTS

PKA-independent effects of FSK-stimulated Cl⁻ secretion in T84 cells

We first tested whether cAMP-stimulated Cl⁻ secretion in T84 cells was exclusively PKA dependent. Cells were grown on transwell supports placed in Ussing chambers containing an HCO₃⁻ free Cl⁻ solution. The PKA inhibitor, H89 (1 μ M), partially inhibited the effect of FSK (10 μ M) (Fig. 1). Similarly, the effect of FSK was partially inhibited by the conventional PKC inhibitor Gö6976 (5 μ M), the PLC inhibitor U73122 (10 μ M), or the intracellular Ca²⁺ chelator BAPTA-AM (25 μ M). However, a high concentration of H89 (50 μ M), which inhibits both PKA and PKC, inhibited \sim 90% of the FSK-stimulated Cl⁻ secretion (Hidaka et al., 1990; Davies et al., 2000; Lochner and Moolman, 2006). Therefore, we further tested whether the combination of 1 μ M H89 and other kinase inhibitors could completely inhibit the FSK-stimulated Cl⁻ secretion. The effects of 1 μ M H89 and 5 μ M Gö6976, of 1 μ M H89 and 25 μ M BAPTA-AM, or of 1 μ M H89 and 10 μ M U73122 were additive. These results suggested that FSK-stimulated Cl⁻ secretion was both PKA and Ca²⁺ dependent, and that the Ca²⁺ effect was additive to the effect of PKA. There was no change in transepithelial resistance before or after BAPTA-AM

addition ($3,234 \pm 117 \Omega \cdot \text{cm}^2$ vs. $3,044 \pm 135 \Omega \cdot \text{cm}^2$, respectively). Similarly, Gö6976, U73122, and H89 did not affect transepithelial resistance (not depicted).

FSK increases [Ca²⁺]_i

We measured the change of [Ca²⁺]_i in T84 cells upon FSK stimulation. The resting level of [Ca²⁺]_i was \sim 150 nM (Fig. 2 A). FSK caused a sustained elevation of [Ca²⁺]_i immediately after its addition ($\Delta[\text{Ca}^{2+}]_i = 42 \pm 10 \text{ nM}$; *P* < 0.05). We then determined the source of the [Ca²⁺]_i increase by measuring [Ca²⁺]_i in the absence of extracellular Ca²⁺ and then after the introduction of 1.8 mM Ca²⁺ to the extracellular medium. Both Ca²⁺ release and entry were observed after FSK addition (Fig. 2 B). The sustained rise in [Ca²⁺]_i depended on extracellular Ca²⁺, whereas the initial rise did not. This increase in [Ca²⁺]_i was blocked by preincubation with the PLC inhibitor U73122 (10 μ M) (Fig. 2 C). Collectively, these results suggested that the FSK-induced [Ca²⁺]_i rise was PLC mediated. The rise in [Ca²⁺]_i further induced the entry of Ca²⁺ across the membrane. The latter fact was further supported by the inhibitory effect of LaCl₃, a nonspecific membrane Ca²⁺ channel blocker (Fig. S1 A). 200 μ M LaCl₃ inhibited the FSK-stimulated Cl⁻ secretion. Similarly, the IP₃-induced Ca²⁺ release inhibitor 2-APB (50 μ M) inhibited the FSK-stimulated Cl⁻ secretion (Fig. S1 B).

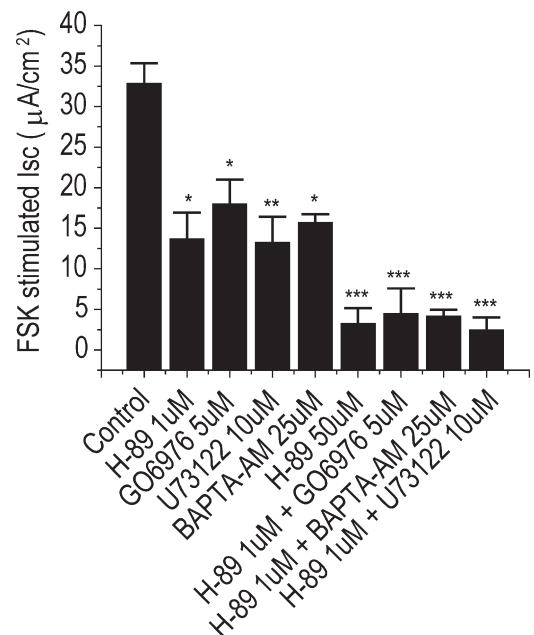


Figure 1. Effect of protein kinase modulators and BAPTA-AM on FSK-stimulated Cl⁻ secretion. Cell monolayers were pretreated with H89, Gö6976, U73122, BAPTA-AM, H89 plus Gö6976, H89 plus BAPTA-AM, or H89 plus U73122 for 30 min with the indicated concentrations. FSK was then added. FSK-stimulated I_{sc} for each condition was derived from the I_{sc} values before and after the addition of FSK. Statistical comparisons between means were performed using Student's *t* test and among means with one-way ANOVA and Student-Newman-Keuls posttest. *, *P* < 0.05; **, *P* < 0.01; ***, *P* < 0.001 compared with FSK control group.

The results from the LaCl_3 and 2-APB experiments demonstrated that Ca^{2+} release from IP_3 -sensitive internal stores and entry from the extracellular milieu may have a role in FSK-stimulated Cl^- secretion.

Expression of Epac in T84 cells

cAMP binds to Epac proteins and subsequently elevates $[\text{Ca}^{2+}]_i$ (de Rooij et al., 1998; Kawasaki et al., 1998). Therefore, as part of establishing a role for Epac in FSK-stimulated Cl^- secretion, we tested whether Epac message or protein is expressed in T84 cells. Using RT-PCR, both Epac1 and Epac2 transcripts were detected (Fig. 3 A).

However, by Western blot, Epac1 but not Epac2 protein was present (Fig. 3 B). This is consistent with the observation that Epac2 is predominately expressed in the brain and adrenal gland, whereas Epac1 has ubiquitous expression (de Rooij et al., 1998; Kawasaki et al., 1998). We further studied the distribution of endogenous Epac1 in T84 cells by immunostaining (Fig. 3 C). Epac1 staining (red) of T84 cells was mostly intracellular, as shown by both the vertical XZ image and the horizontal XY image. A control experiment with only secondary antibody did not have specific staining (not depicted).

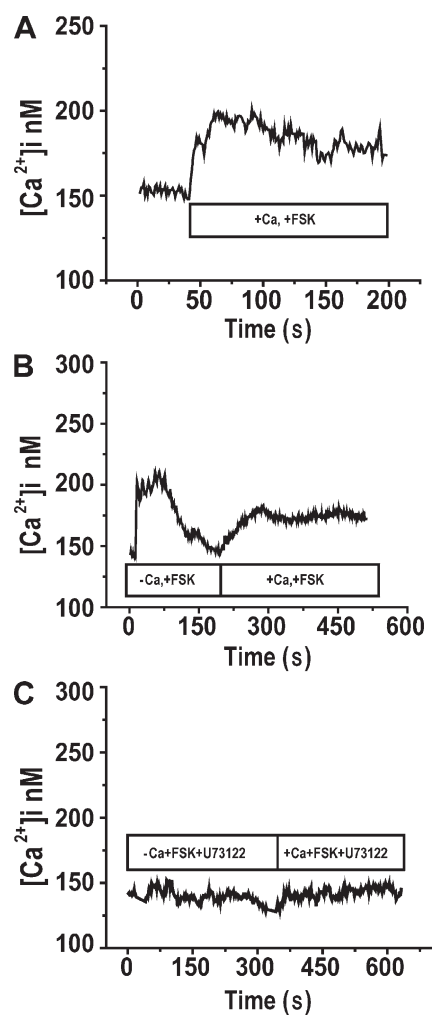


Figure 2. Measurement of $[\text{Ca}^{2+}]_i$ in T84 cells. (A) Cells were loaded with Fura2-AM at 37°C in the presence of 1.2 mM of extracellular Ca^{2+} . After 30 min of de-esterification in the presence of 5 μM indomethacin, cell monolayers were used for $[\text{Ca}^{2+}]_i$ measurement at room temperature in the presence of 1.8 mM of extracellular calcium and challenged with 10 μM FSK as indicated ($n = 3$). (B) $[\text{Ca}^{2+}]_i$ was measured in cells challenged with 10 μM FSK initially in the absence of extracellular Ca^{2+} , followed by reintroduction of 1.8 mM of extracellular Ca^{2+} . (C) $[\text{Ca}^{2+}]_i$ was measured in cells in the absence or presence of extracellular Ca^{2+} by preincubating with 10 μM U73122 during the 30 min of de-esterification. FSK was then added ($n = 3$).

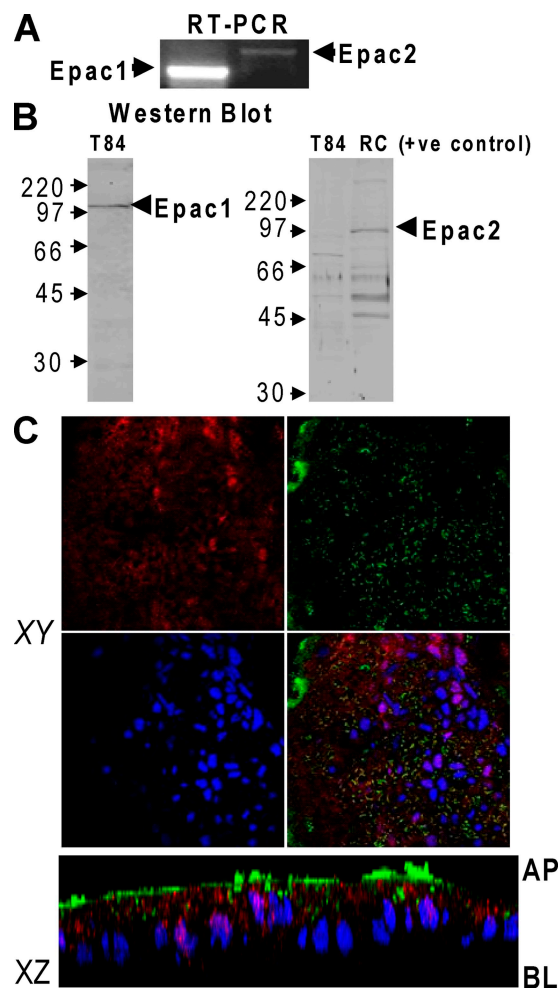


Figure 3. Expression and localization of Epac in T84 cells. (A) Epac1 and Epac2 message was amplified by RT-PCR from T84 cell total RNA ($n = 6$). (B) Epac1 (≈ 105 kD) and Epac 2 (≈ 100 kD) expression in total cell lysate of T84 was analyzed by Western blot. Total rat cerebellum (RC) lysate was used as positive control. A representative blot is shown ($n = 5$). (C) T84 cells were stained with anti-Epac₁₋₇₀ (red), nucleus with Hoechst (blue), and apical surface with wheat germ agglutinin (green) as described in Materials and methods. Vertical (XZ) and horizontal (XY) confocal microscopy sections showed the subcellular distribution of Epac1 in T84 cells. AP, apical side; BL, basolateral side. Images shown are representative of three similar experiments.

Role of Epac in FSK-stimulated Cl^- secretion in T84 cells

To establish a link from cAMP to PLC/ $[\text{Ca}^{2+}]_i$ /PKC signaling and to support a role for Epac in Cl^- secretion, we determined whether 8-pCPT-2'-O-Me-cAMP, an Epac agonist, could stimulate Cl^- secretion in T84 cells. As shown in Fig. 4 A, 50 μM 8-pCPT-2'-O-Me-cAMP stimulated Cl^- secretion. 8-pCPT-2'-O-Me-cAMP had been shown to selectively stimulate Epac at 50–200 μM (Kang et al., 2003; Holz, 2004; Yip, 2006). We found 100–200 μM 8-pCPT-2'-O-Me-cAMP did not further enhance Cl^- secretion in T84 cells (not depicted), suggesting that 50 μM 8-pCPT-2'-O-Me-cAMP already produced a maximal effect. This increase in I_{sc} was completely blocked by pretreatment of the cells with 25 μM BAPTA-AM, but not with 1 μM H89. Therefore, $[\text{Ca}^{2+}]_i$, but not PKA, mediated the effect of 8-pCPT-2'-O-Me-cAMP. We hypothesized that if the Epac/PLC/ $[\text{Ca}^{2+}]_i$ /PKC pathway contributed to the PKA-independent component of FSK-stimulated Cl^- secretion, the combined effects of PKA and Epac on Cl^- secretion in T84 cells would be additive. As shown in Fig. 4 B, the PKA agonist Sp-8-pCPT-cAMP (20 μM) (Christensen et al., 2003) stimulated Cl^- secretion. Gradual increases in the concentration of Sp-8-pCPT-cAMP to 100 μM did not further stimulate Cl^- secretion (not depicted). However, the addition of the Epac activator (50 μM) further stimulated Cl^- secretion. The stimulatory effect of 20 μM Sp-8-pCPT-cAMP and 50 μM 8-pCPT-2'-O-Me-cAMP on Cl^- secretion was additive.

We tested whether 10 μM FSK or 50 μM 8-pCPT-2'-O-Me-cAMP was capable of activating Rap2 in T84 cells because activation of Rap2 leads to the activation of PLC ϵ and increased $[\text{Ca}^{2+}]_i$ (Evellin et al., 2002). As shown in Fig. 5 A, a 20-min treatment of either FSK or 8-pCPT-2'-O-Me-cAMP increased the amount of GTP-Rap2. This result further suggested that Epac was activated by FSK or 8-pCPT-2'-O-Me-cAMP, and that activation of

Epac subsequently led to activation of Rap2 and elevation of $[\text{Ca}^{2+}]_i$, the latter event caused by selective activation of Epac with 8-pCPT-2'-O-Me-cAMP, leading to a rise of $[\text{Ca}^{2+}]_i$ ($\Delta[\text{Ca}^{2+}]_i = 45 \pm 7$ nM; $n = 3$) (Fig. 5 B).

Effect of Epac on apical Cl^- conductance

Because Cl^- secretion involves the coordinated functions of apical Cl^- channels and the basolateral membrane transporters, such as Na/K/ATPase, $\text{Na}^+/\text{K}^+/\text{2Cl}^-$, and K channels, and the effect of Epac on Cl^- secretion appears to be moderate, we addressed whether Epac has any effect on apical Cl^- channels and whether this effect is enhanced in cells with the basolateral membrane permeabilized. I_{Cl} was measured in T84 monolayers treated with 50 $\mu\text{g}/\text{ml}$ nystatin on the basolateral membrane. The permeabilized cells were exposed to a basolateral to apical Cl^- gradient (Mun et al., 1998). Treatment with 10 μM FSK led to a brisk and sustained increase in I_{Cl} , which represented an activation of apical chloride channels (Fig. 6 A). After the maximal effect of FSK was obtained, the addition of 8-pCPT-2'-O-Me-cAMP had no additional effect on I_{sc} (not depicted). The FSK effect was partially inhibited by BAPTA-AM (Fig. 6 A). 8-pCPT-2'-O-Me-cAMP also increased apical I_{Cl} in basolaterally permeabilized cells. In contrast to FSK, the 8-pCPT-2'-O-Me-cAMP-stimulated apical I_{Cl} was completely inhibited by BAPTA-AM (Fig. 6 B).

Effect of BAPTA and U73122 on VIP- and 8-Br-cAMP-stimulated Cl^- secretion in T84 cells

VIP acts through a G protein-coupled receptor that activates Gs/adenylylase to increase intracellular cAMP. The cAMP analogue 8-Br-cAMP activates PKA and possibly Epac as well (de Rooij et al., 1998; Kawasaki et al., 1998). We tested whether these two agents stimulated Cl^- secretion in a manner similar to FSK. As shown in Fig. S2 A, BAPTA-AM and U73122 significantly

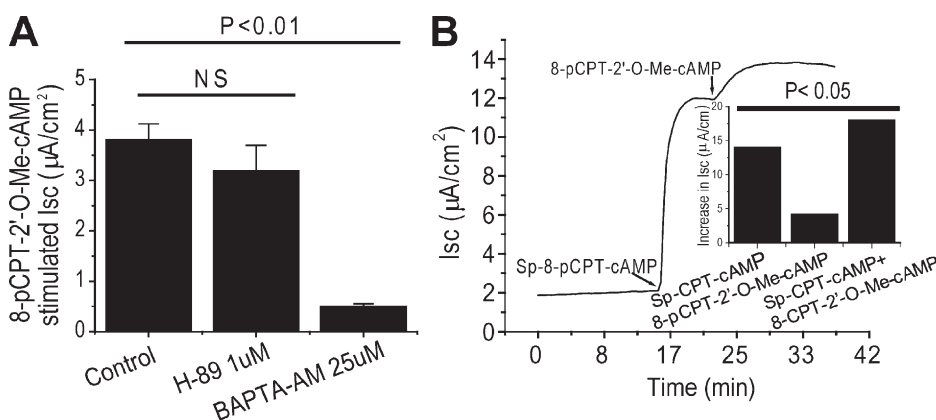


Figure 4. Direct activation of Epac with 8-pCPT-2'-O-Me-cAMP-stimulated Cl^- secretion in T84 cells. (A) 50 μM 8-pCPT-2'-O-Me-cAMP was added to the basolateral membrane of control cells or cells preincubated with 1 μM H89 or 25 μM BAPTA-AM for 30 min. 8-pCPT-2'-O-Me-cAMP-stimulated I_{sc} was derived from the I_{sc} values before and after the addition of 8-pCPT-2'-O-Me-cAMP. Values are means \pm SEM ($n = 5$). Statistical comparisons between means were performed using Student's t test. NS, not significant. (B) Additive effects of Sp-8-pCPT-cAMP and 8-pCPT-2'-O-Me-cAMP

on Cl^- secretion in T84 cells. 20 μM Sp-8-pCPT-cAMP was added to the basolateral membrane. This induced a sustained Cl^- secretion. 50 μM 8-pCPT-2'-O-Me-cAMP was subsequently added, and this caused a further increase in I_{sc} . Values are means \pm SE ($n = 6$). The inset shows the individual effect of 20 μM Sp-CPT-cAMP and 50 μM 8-pCPT-2'-O-Me-cAMP and their additive effect on Cl^- secretion in T84 cells. Statistical comparisons between means were performed using Student's t test.

reduced the VIP (100 nM) -stimulated Cl^- secretion. Similarly, BAPTA-AM and U73122 also inhibited 8-Br-cAMP (100 μM) -stimulated Cl^- secretion (Fig. S2 B). These findings suggested that a rise of $[\text{Ca}^{2+}]_i$ is involved in G protein-coupled receptor-mediated and the cAMP-dependent process of Cl^- secretion in T84 cells.

Role of Epac in FSK-stimulated net ion transport in mouse ileum

To determine whether the stimulation of Cl^- secretion by Epac1 is a general mechanism of regulating intestinal Cl^- secretion, we determined that Epac1 was expressed in different segments of mouse intestine, including duodenum, jejunum, ileum, and colon, suggesting that this pathway could be activated along the intestine (Fig. 7 A). 8-pCPT-2'-O-Me-cAMP stimulated net ion transport in mouse ileum, and this was not inhibited by 1 μM H89 but was inhibited by BAPTA-AM treatment (Fig. 7 B). The 8-pCPT-2'-O-Me-cAMP-stimulated I_{Cl} in mouse ileum, with the basolateral membrane permeabilized with nystatin, was not inhibited by the CFTRinh-172 (Fig. 7 C).

Epac1 silencing in T84 cells

To further establish the role of Epac1 in FSK-stimulated Cl^- secretion, lentivirus containing shRNA against Epac1

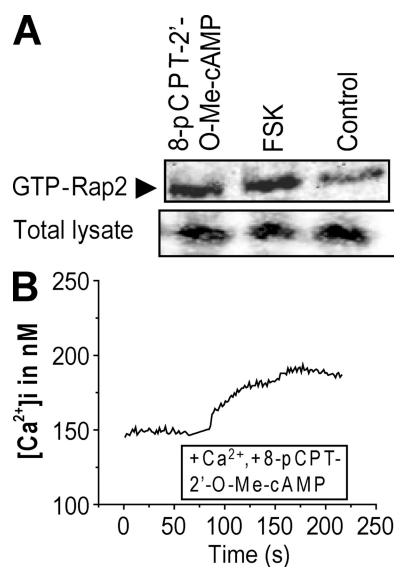


Figure 5. Activation of Rap2 by FSK and 8-pCPT-2'-O-Me-cAMP in T84 cells. (A) Cells were stimulated for 20 min without (control) or with either 10 μM FSK or 50 μM 8-pCPT-2'-O-Me-cAMP, followed by extraction of GTP-loaded Rap2 with glutathione-S-transferase-RALGDS-RBD fusion protein. Samples were analyzed by Western blotting with an anti-Rap2 antibody. A representative Western blot of three experiments is shown. (B) 8-pCPT-2'-O-Me-cAMP elevated $[\text{Ca}^{2+}]_i$ in T84 cells. Cells were loaded with Fura2-AM at 37°C in the presence of extracellular Ca^{2+} . After 30 min of de-esterification in the presence of 2 μM indomethacin, cell monolayers were subjected to $[\text{Ca}^{2+}]_i$ measurement at room temperature in the presence of 1.8 mM of extracellular Ca^{2+} and challenged with 50 μM 8-pCPT-2'-O-Me-cAMP as indicated ($n = 3$).

was used to silence Epac1 protein expression in T84 cells. We used three different TRC shRNA constructs, which had not previously been experimentally validated (as described in Materials and methods). Lentiviral particles were prepared from each shRNA construct and transduced into T84 cells. Cells resistant to puromycin were selected and characterized by Western blot. Of the three shRNA constructs tested, only the constructs 228

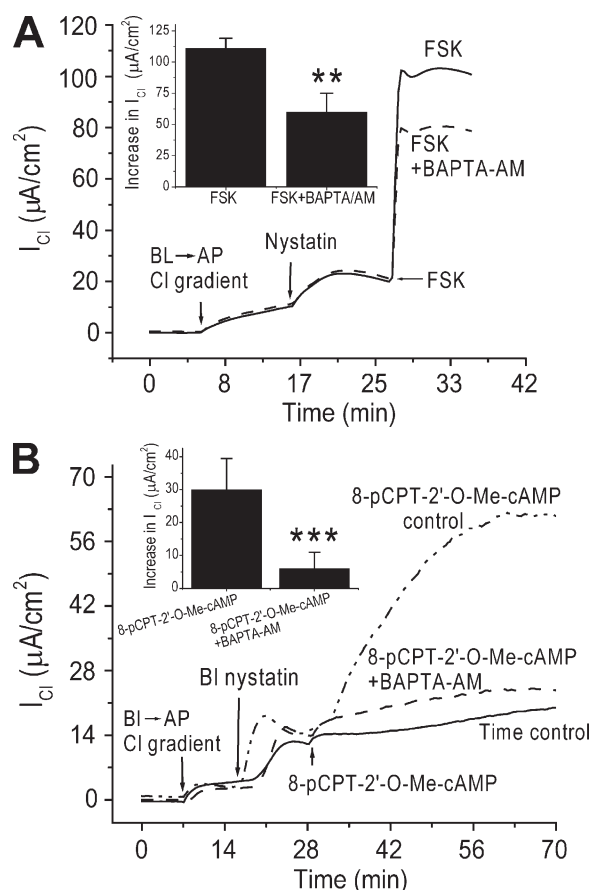


Figure 6. Effect of FSK and 8-pCPT-2'-O-Me-cAMP on apical Cl^- conductance in T84 cells permeabilized by nystatin on the basolateral membrane. Cells were equilibrated with Cl^- free/high K^+ buffer. After equilibration, the basolateral solution was replaced with a high Cl^- /high K^+ solution, and this imposed a basolateral to apical Cl^- gradient. When the steady state was reached, 50 $\mu\text{g}/\text{ml}$ nystatin was added to permeabilize the basolateral membrane. After the basal I_{Cl} subsided, 10 μM FSK (A) or 50 μM 8-pCPT-2'-O-Me-cAMP (B) was added to the permeabilized basolateral membrane. These induced a robust increase of I_{Cl} . To prevent the elevation of $[\text{Ca}^{2+}]_i$, cells were incubated with 25 μM BAPTA-AM for 30 min before the addition of FSK or 8-pCPT-2'-O-Me-cAMP. The FSK effect was partially inhibited by BAPTA-AM (A; inset). In contrast, 8-pCPT-2'-O-Me-cAMP-stimulated apical Cl^- conductance was completely inhibited by BAPTA-AM (B; inset). A representative tracing is shown for each experiment. The increase in I_{Cl} was derived from the I_{Cl} value before and after the addition of FSK ($n = 3$) or 8-pCPT-2'-O-Me-cAMP ($n = 5$). Values are means \pm SEM. Statistical comparisons between means were performed using Student's t test. **, $P < 0.01$; ***, $P < 0.001$ compared with control group.

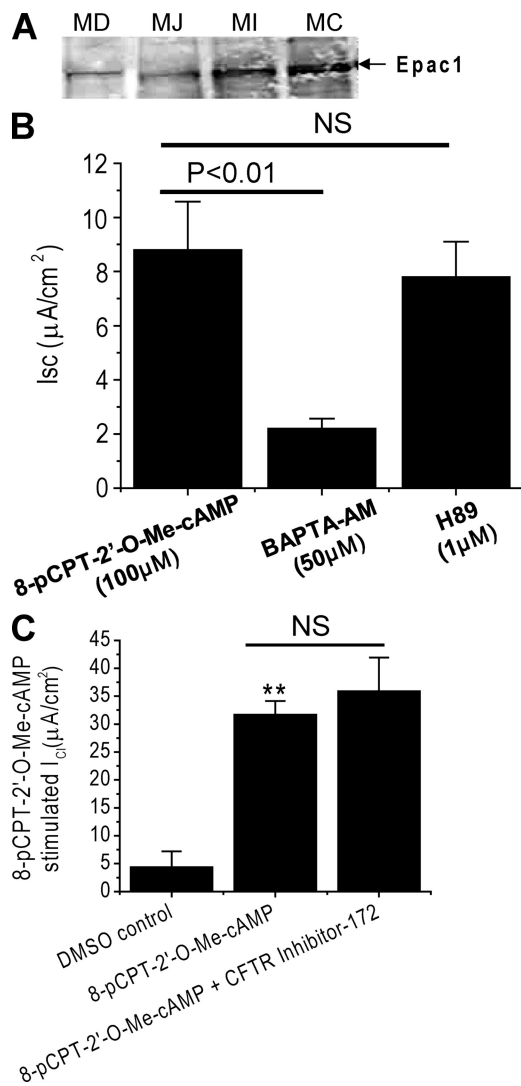


Figure 7. Western blot of total lysates from mouse intestinal mucosal scrapings. (A) Epac1 is expressed in different segments of the intestine, including duodenum (MD), jejunum (MJ), ileum (MI), and colon (MC; $n = 3$). (B) Activation of Epac with 8-pCPT-2'-O-Me-cAMP-stimulated net ion transport in mouse ileal sheets (ex vivo). 100 μM 8-pCPT-2'-O-Me-cAMP was added to the basolateral membrane of control mouse ileum or ileum preincubated with 1 μM H89 or 25 μM BAPTA-AM for 30 min. The 8-pCPT-2'-O-Me-cAMP-stimulated I_{sc} was calculated from the I_{sc} values before and after the addition of 8-pCPT-2'-O-Me-cAMP. H89 had no effect on 8-pCPT-2'-O-Me-cAMP-stimulated I_{sc} , whereas BAPTA-AM inhibited the current. Values are means \pm SEM ($n = 5$). (C) Ex vivo apical I_{Cl} measurement in mouse ileum permeabilized by nystatin on the serosal side. Tissues were equilibrated with Cl^- free/high K^+ buffer. After equilibration, the basolateral solution was replaced with a high Cl^- /high K^+ solution, which imposed a basolateral to apical Cl^- gradient. When the steady state was reached, 50 $\mu g/ml$ nystatin was added to permeabilize the serosal membrane. 8-pCPT-2'-O-Me-cAMP induced a robust increase of I_{Cl} , which was insensitive to the CFTRinh-172. Data are expressed as the mean \pm SE ($n > 3$). **, $P = 0.01$ compared with the DMSO control. Statistical comparisons between means were performed using Student's t test. NS, not significant.

(referring to the last three digits of the TRC number) and 231 were able to reduce the expression of Epac1 in T84 cells by 89 and 76%, respectively, as determined by Western blot densitometry. However, the construct 230 failed to silence Epac1 (Fig. 8 A). There was no change in the expression of CFTR protein between the wild-type cells, vector-transduced cells, and cells transduced with putative Epac1 shRNA constructs. The functional consequence of Epac1 silencing with respect to FSK-stimulated Cl^- secretion was tested using these cell lines. As shown in Fig. 8 B, the Epac1KDT84cst228 and Epac1KDT84cst231 cells exhibited only ~ 43 –50% of FSK-stimulated Cl^- secretion compared with wild-type and vector-transduced cells. In contrast, the Epac1KDT84cst230 cells having the shRNA construct 230 that failed to silence Epac1 protein responded to FSK with a similar magnitude of Cl^- secretion as wild-type and vector-transduced cells. FSK-stimulated Cl^- secretion in Epac1KDT84cst228 cells was inhibited by 1 μM H89, but not by U73122 and BAPTA-AM (Fig. 8 C), confirming that in the absence of Epac1, FSK-stimulated Cl^- secretion was completely PKA dependent. FSK and the Epac activator also failed to elevate $[Ca^{2+}]_i$ in these Epac-silenced cells (not depicted).

Epac-mediated chloride currents are not caused by CFTR
To further confirm that Epac1-mediated Cl^- secretion in T84 cells was not due to CFTR, we transiently transfected CHO cells that express endogenous Epac1 with a CFTR construct. Then, Cl^- currents were recorded in the whole cell configuration (Lorenowicz et al., 2006). As shown in Fig. S3 (A–C), 100 μM 8-pCPT-2'-O-Me-cAMP had no effect on current amplitudes (233.9 ± 65.2 pA vs. 203.7 ± 58.3 pA; $P = 0.29$), whereas subsequent application of a CFTR-stimulating cocktail of 100 μM cpt-cAMP plus 10 μM FSK activated large, linear CFTR currents ($1,334.7 \pm 250.5$ pA; $P \leq 0.005$) (Fig. S3, A and B). The cpt-cAMP/FSK-activated currents were inhibited by the application of 10 μM CFTR inh-172 ($I_{pA} = 392.7 \pm 149.7$; $P \leq 0.01$). The cpt-cAMP/FSK-activated Cl^- currents and the inhibition by 10 μM CFTRinh-172 demonstrated that the Cl^- conductance stimulated by cpt-cAMP/FSK was specifically a CFTR-mediated conductance.

Biophysical properties of the Epac-stimulated I_{Cl}
We characterized the biophysical properties of the secretory currents activated by Epac. We took advantage of the basolateral-permeabilized membrane protocol to isolate the channel currents at the apical surface, allowing a description of the I-V relationship and measurement of the reversal potential. In Fig. 9 A, we plotted the current against the clamped, stepped voltages of T84 monolayers with permeabilized basolateral membranes in the presence of 50 μM 8-pCPT-2'-O-Me-cAMP. The recorded currents had significant inward rectification

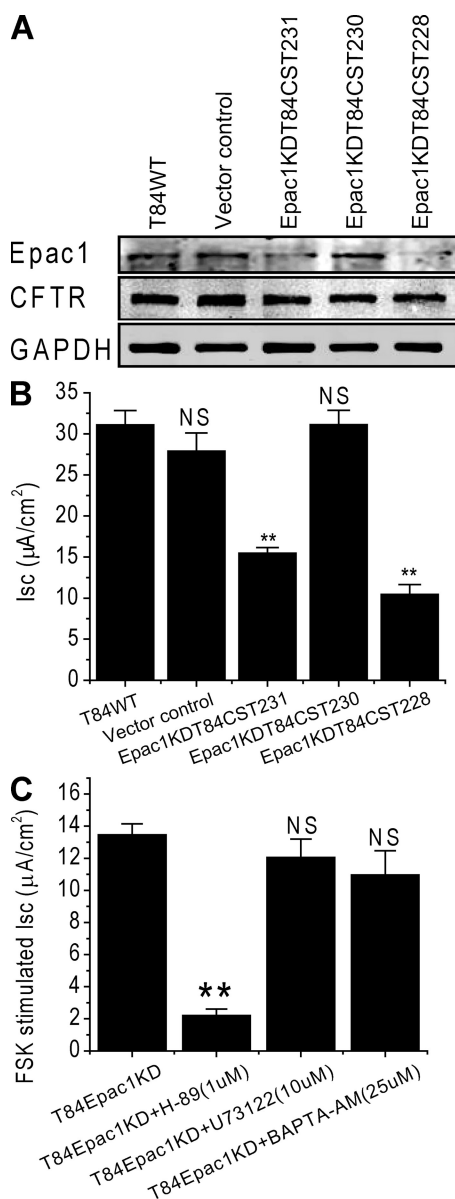


Figure 8. Epac1 silencing in T84 cells. (A) Western blot analysis of Epac1 expression in total cell lysate of wild-type T84 (T84-WT), vector control, and Epac1 shRNA-transduced cells (EpacKDT84CST228, EpacKDT84CST230, and EpacKDT84CST231). The amount of Epac1 protein was decreased by 76% in EpacKDT84CST228 and 89% in EpacKDT84CST231 cells, as determined by densitometry and normalized to glyceraldehyde-3-phosphate dehydrogenase (GAPDH) ($n = 4$). EpacKDT84CST230 expressed the same amount of Epac1 protein as wild-type T84 cell and thus was used as a negative control for silenced cells. There was no change in CFTR expression. (B). EpacKDT84CST228 and EpacKDT84CST231 cells responded to FSK with a stimulated Cl^- secretion having only half the magnitude as that of wild-type and vector-transduced cells ($n = 5$). In contrast, EpacKDT84CST230 responded to FSK with a stimulated Cl^- secretion similar to wild-type cells. Statistical comparisons among means were performed with one-way ANOVA and Student-Newman-Keuls posttest. **, $P < 0.01$ compared with T84WT. (C) FSK-stimulated Cl^- secretion in EpacKDT84CST228 cells was inhibited by 1 μM H89, but not by U73122 and BAPTA ($n = 5$). Values are means \pm SEM ($\mu\text{A}/\text{cm}^2$). Statistical comparisons between means were performed

with a reversal potential of 39 mV. The only non-balanced ion/anion was Cl^- with a Nernst potential of 90.0 mV, somewhat dissimilar from that of the Nernst potential of the Epac-stimulated current. This discrepancy might be due, in part, to the small amplitude of the recorded current, suggesting that the Epac activator did not fully stimulate the Cl^- current. This drawback, along with our inability to use large amounts of the 8-pCPT-2'-O-Me-cAMP compound because of its scarcity, led us to rely on FSK activation of the Epac currents with and without CFTRinh-172. Fig. 9 B reveals that outward FSK-activated currents (black squares) had large amplitudes and were somewhat linear, but the apical application of the CFTRinh-172 decreased the current amplitude and changed the shape of the I-V relationship. The FSK plus CFTRinh-172 currents were inwardly rectifying, similar to the currents activated by 8-pCPT-2'-O-Me-cAMP (Fig. 9 B). In either case, it is important to note that K^+ ions at nonzero potentials could possibly be contributing to the I-V shape through yet unknown apical K^+ channels, although unlikely in secretory T84 cells.

We next measured the reversal potentials for the FSK-activated currents with or without the CFTRinh-172 and with or without a steep basal to apical Cl^- gradient (Fig. 9 C). The FSK-activated chloride current had a reversal potential of 76 mV ($E_{\text{rev}} \text{Cl}^- = 90.0$ mV), indicating that the largest apical ion conductance was a Cl^- conductance (all other permeant ions had a zero Nernst potential), a conductance that had been shown many times to be largely mediated by CFTR. The application of the CFTRinh-172 shifted the reversal potential to 52 mV. The shift represented the loss of the Cl^- conductance through CFTR channels on the apical membrane, suggesting that the remaining current was the Epac-activated Cl^- conductance and a sizable but unchanging leak current ($E_{\text{leak}} = 0$ mV). Balancing Cl^- on either side of the apical membrane (new $E_{\text{Cl}^-} = 0$ mV) shifted the reversal potential to 6 mV, demonstrating the Epac-mediated current was a Cl^- current. Using Fick's first law, we next calculated the absolute permeabilities of Cl^- : $P_{\text{Cl}^-} = J_{\text{Cl}^-} / ([\text{Cl}^-]_{\text{in}} - [\text{Cl}^-]_{\text{out}})$ (mmol/cm²s) / (mmol/cm³), where $J_{\text{Cl}^-} = (I_{\text{Cl}^-} \text{ at } 0 \text{ mV}) / \text{Faraday constant}$. The calculated P_{Cl^-} for the FSK-activated currents was 16.04×10^{-6} , very similar to that reported previously ($13.1 \pm 1.8 \times 10^{-6}$; Huflejt et al., 1994) also in T84 cells. The CFTRinh-172-inhibited current had a $P_{\text{Cl}^-} = 8.61 \times 10^{-6}$, a sizable Cl^- permeability and larger than that measured for carbachol-activated chloride currents (Huflejt et al., 1994). Finally, we investigated the permeability of the Epac-mediated Cl^- currents (Fig. 9 D). We substituted either I^- or Br^- on the basolateral side and measured the I_{sc} with

using Student's t test. NS, not significant. **, $P < 0.01$ compared with control.

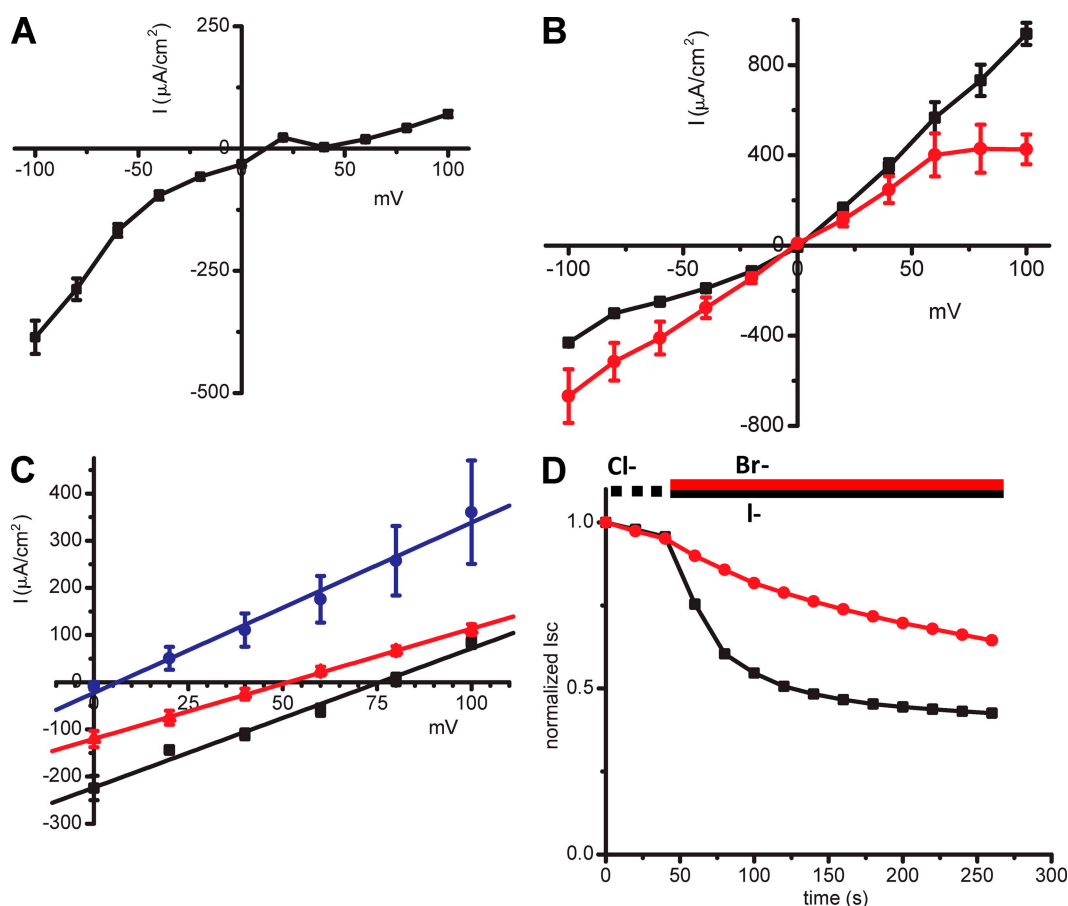


Figure 9. Biophysical characterization of FSK-activated, Epac-mediated I_{sc} current. (A) I-V plot of the 8-pCPT-2'-O-Me-cAMP-stimulated current of nystatin-permeabilized T84 cells with basal to apical ($\Delta 145$ mM) Cl^- gradient. Currents are portrayed using the physiological convention, where membrane potential (V) = basolateral (V1) – apical (V2), possible here because the basolateral membrane is permeabilized to Cl^- . Data are means \pm SEM ($n = 6$). See Materials and methods for complete description of this experiment. (B) I-V plot of current recordings of nystatin-permeabilized T84 cells treated with 10 μ M FSK (black squares) or 10 μ M FSK plus 5 μ M CFTRinh-172 (red circles) under symmetrical (basal/apical) Cl^- gradient (data are means \pm SEM; $n = 2-8$). (C) Reversal potential measurements from voltage-clamped basolaterally permeabilized T84 cells: I-V relationships of outward currents with linear fits for apical membranes treated with FSK (black squares; $R^2 = 0.98931$ and $E_{rev} = 76$; $n = 5$), FSK plus CFTRinh-172 (red triangles; $R^2 = 0.99942$ and $E_{rev} = 52$; $n = 5$), or FSK plus CFTRinh-172 plus symmetrical Cl^- (blue circles; $R^2 = 0.98337$ and $E_{rev} = 6$; $n = 3$). (D) Halide selectivity: representative I_{sc} recordings from permeabilized T84 cells treated with FSK plus CFTRinh-172. The apical and basolateral sides were bathed with a Cl^- -containing solution, an equal molar of Br^- or I^- was substituted on the basal side, and the I_{sc} was recorded.

basolateral-permeabilized membranes. We found that Cl^- was more permeable than either I^- or Br^- , with a selectivity sequence of $Cl^- > Br^- > I^-$ and relative permeabilities of $P_{Cl^-}/P_{Cl^-} = 1$, $P_{Br^-}/P_{Cl^-} = 0.9$, and $P_{I^-}/P_{Cl^-} = 0.6$. The anion permeability through nystatin pores is based on hydrated ion radius (Cass et al., 1970), and Cl^- , Br^- , and I^- have essentially the same hydrated radius (3.32, 3.30, and 3.31 Å) (Conway, 1981) and thus predictive similar nystatin permeabilities.

To identify blockers of the apical Cl^- conductance involved in the Epac-mediated Cl^- secretion, the 8-pCPT-2'-O-Me-cAMP-stimulated I_{Cl} was challenged with 5 μ M of the CFTRinh-172 (Ma et al., 2002; Factor et al., 2007) or 100 μ M glibenclamide (Schultz et al., 1996; Sheppard and Robinson, 1997). Other inhibitors added were 100 μ M niflumic acid, which inhibits the calcium-activated Cl^-

channel (CaCC), 100 μ M zinc (Zn^{2+}), and 1 mM cadmium chloride (Cd^{2+}), which inhibits the voltage-gated Cl^- channel isoform 2 (CIC2). The lack of effect of these inhibitors suggested that CFTR, CaCC, and CIC2 were not responsible for Epac-mediated Cl^- secretion (Fig. 10 A). To ascertain that cAMP-stimulated Cl^- secretion occurs through two different Cl^- channels, we measured I_{Cl} in basolaterally permeabilized T84 cells in the presence of either CFTRinh-172 plus DIDS or CFTRinh-172 plus NPPB. Fig. 10 B shows that the combined effect of CFTRinh-172 along with either DIDS or NPPB was greater compared with CFTRinh-172 alone. Thus, these two inhibitors partially inhibited a component of the cAMP-stimulated Cl^- secretion in intact T84 cells (not depicted; Merlin et al., 1998). Interestingly, we have found that the cAMP-stimulated apical I_{Cl} was completely inhibited by

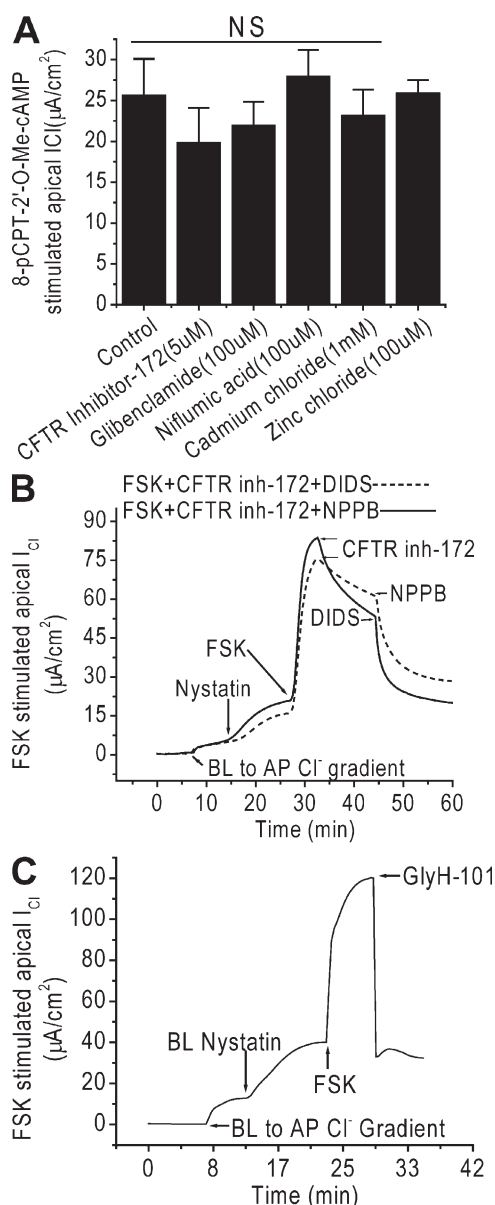


Figure 10. Pharmacological profile of the Cl^- channel blockers in basolaterally permeabilized T84 cells. (A) Effect of channel blockers on 8-pCPT-2'-O-Me-cAMP-stimulated apical Cl^- conductance. 5 μM CFTRinh-172, 100 μM glibenclamide, 100 μM niflumic acid, or 1 mM cadmium chloride ($CdCl_2$) was applied after maximum Cl^- currents in the presence of 50 μM 8-pCPT-2'-O-Me-cAMP (data are mean \pm SEM; $n = 3-5$). NS, not significant. (B) Effects of DIDS or NPPB on FSK-stimulated I_{Cl} in the presence of CFTRinh-172. Representative traces showing that 100 μM DIDS and 100 μM NPPB inhibited the FSK-stimulated, CFTRinh-172-insensitive Cl^- current (Epac mediated) in basolaterally permeabilized T84 cells. (C) Effect of 10 μM GlyH-101 on FSK-stimulated I_{Cl} in basolaterally permeabilized T84 cells. Representative trace showing that GlyH-101 completely inhibited FSK-stimulated apical I_{Cl} ($n = 3$).

GlyH-101 (Fig. 10 C), a previously considered CFTR blocker but now known to also block $CaCCs$ (Hartzell et al., 2009).

DISCUSSION

PKA has been regarded as the major and only effector of cAMP in modulating CFTR function in the apical membrane of intestinal and airway cells (Vajanaphanich et al., 1995; Barrett, 2000; Huang et al., 2000; Boucher, 2007; Thelin and Boucher, 2007). However, Merlin et al. (1998) showed that FSK is capable of elevating $[Ca^{2+}]_i$ in intestinal T84 cells, in addition to increasing intracellular cAMP concentrations (Merlin et al., 1998; Holz, 2004). This suggests that $[Ca^{2+}]_i$ might also be involved in intestinal Cl^- secretion as a consequence of FSK stimulation. The mechanism by which FSK elevates $[Ca^{2+}]_i$ has not been clear. Epac is a cAMP-binding protein that transduces cAMP signaling into increases in $[Ca^{2+}]_i$ (Schmidt et al., 2001). Because both PKA and Epac are broadly expressed in many tissues and are activated by binding to cAMP with similar affinity (de Rooij et al., 1998; Kawasaki et al., 1998; Schmidt et al., 2001), an increase in intracellular cAMP will likely lead to activation of both PKA and Epac.

Our data showed that both PKA and PLC/ $[Ca^{2+}]_i$ /PKC pathways were involved in FSK-stimulated Cl^- secretion and their effects were additive. It was shown that H89 inhibits PKA in nanometer concentrations ($IC_{50} = 48$ nM), whereas at micrometer ($IC_{50} = 14$ μM) concentrations, it inhibits PKC as well (Chijiwa et al., 1990; Hidaka et al., 1990; Hidaka and Kobayashi, 1992; Muroi and Suzuki, 1993; Davies et al., 2000; Lochner and Moolman, 2006). Thus, 1 μM H89 has been used to selectively inhibit PKA, for example, in studies demonstrating adenosine-induced PKA activation of K^+ channel currents in arterial myocytes (Kleppisch and Nelson, 1995) and for distinguishing between PKA-dependent and -independent apical exocytosis of aquaporin-2 in renal inner medullary collecting duct cells (Yip, 2006). In our studies, 1 μM H89 was used to inhibit the PKA-dependent component of FSK-stimulated Cl^- secretion. It was found that 1 μM H89 only partially inhibited FSK-stimulated Cl^- secretion, which was also partially inhibited by U73122, Gö6976, and BAPTA-AM. The effects of H89 and Gö6976, of H89 and BAPTA-AM, or of H89 and U73122 were additive. These results suggested the presence of a Ca^{2+} -sensitive, PKA-independent component of Cl^- secretion. The cAMP secretagogue, VIP, and 8-Br-cAMP had the same effect as FSK. Furthermore, FSK increased $[Ca^{2+}]_i$ in T84 cells. Thus, our observation confirmed the finding of Merlin et al. (1998), that FSK induced a moderate increase in $[Ca^{2+}]_i$. It is worthwhile to note that FSK/cAMP is also found to increase $[Ca^{2+}]_i$ in chicken enterocytes (Semrad and Chang, 1987) and intestinal HT29 cells (Denning et al., 1994). In addition, apical adenosine, acting via cAMP, has recently been shown to regulate basolateral Ca^{2+} -activated K channels in Calu-3 cells via PLC- and Ca^{2+} -dependent signaling pathways (Wang et al., 2008). FSK/cAMP is

also able to mobilize $[Ca^{2+}]_i$ in inner medullary collecting duct cells (Yip, 2006), rat cardiac myocytes (Pereira et al., 2007), and HEK293 cells (Schmidt et al., 2001) and increases Ca^{2+} -induced Ca^{2+} release in pancreatic β cells (Dyachok et al., 2004; Dyachok and Gylfe, 2004; Holz, 2004). These studies also support the link between cAMP with Ca^{2+} mobilization as observed in our studies.

Upon binding cAMP, Epac activates Rap GTPases, which stimulate PLC ϵ and mobilize $[Ca^{2+}]_i$ from intracellular stores (Schmidt et al., 2001). PLC is involved in FSK, VIP, or 8-Br-cAMP increases in Cl^- conductance because the conductance is partially inhibited by the PLC inhibitor, U73122. The effect of Epac and FSK on $[Ca^{2+}]_i$ is completely abolished by U73122. Among various PLC isoforms, PLC ϵ is an effector of Ras. Association of Ras and Rho proteins with the Ras-binding domains of PLC ϵ activates the phospholipase activity of the enzyme (Maly et al., 2007). The direct involvement of Epac in Cl^- secretion was indicated by the use of the Epac activator, which activates Rap2, elevates $[Ca^{2+}]_i$, and stimulates Cl^- secretion. 8-pCPT-2'-O-Me-cAMP also stimulated net ion transport in mouse ileum independently of PKA. Furthermore, other evidence confirming the role of the Epac pathway after increases in cAMP came from our studies on Epac1KDT84cst228 and Epac1KDT84cst231 cells that exhibited >75% reduction in expression of Epac1 protein and responded to FSK-stimulated Cl^- secretion with only half the magnitude as that of wild-type and vector-transduced cells. Most importantly, this reduction in I_{sc} response to FSK was not due to a change in CFTR protein. Our studies also found that the construct TRCN000047230 failed to silence Epac1; therefore, Epac1KDT84cst230 cells were considered a negative control in addition to the vector-transduced cells. FSK-stimulated Cl^- secretion in Epac1KDT84cst228 cells was completely dependent on PKA, no longer dependent on PLC, and insensitive to BAPTA-AM treatment. Thus, these studies provide compelling evidence that Epac contributed to the FSK-stimulated Cl^- secretion.

Previous studies by Vajanaphanich et al. (1995) demonstrated a synergistic Cl^- secretion in T84 cells in response to simultaneous elevation of cAMP and Ca^{2+} . Based on the model of intestinal Cl^- secretion, which involves basolateral $Na^+/K^+/2Cl^-$ cotransporter and K^+ channels as well as apical Cl^- channels, possible mechanisms of synergism include cooperative effects of cAMP and Ca^{2+} on the apical Cl^- conductance and/or stimulated opening of Ca^{2+} -regulated basolateral K channel (Anderson and Welsh, 1991; Reenstra, 1993; Barrett and Keely, 2000). Therefore, we tested whether sequential addition of Sp-8-pCPT-cAMP and 8-pCPT-2'-O-Me-cAMP would result in synergistic response to Cl^- secretion. Our result suggested that the effects of Sp-8-pCPT-cAMP and 8-pCPT-2'-O-Me-cAMP were additive. Because the order of addition might affect the outcome (Vajanaphanich

et al., 1995), we challenged T84 cells with the addition of 8-pCPT-2'-O-Me-cAMP followed by Sp-8-pCPT-cAMP, and the same result was obtained (not depicted). In addition, when the maximal effect of FSK alone was obtained, the Epac pathway appeared to have been fully activated, as there was no additional effect on I_{sc} by Epac stimulator addition. To reconcile the synergistic effect on Cl^- secretion by the combined addition of cAMP and carbachol and the additive effect of Sp-8-pCPT-cAMP and the Epac activator, it should be pointed out that the Ca^{2+} -elevating agent carbachol acts through the Gq-coupled receptor. Different pools of intracellular Ca^{2+} might have been mobilized by Epac and carbachol, and consequently, their downstream signaling events and effects on Cl^- secretion would be predicted to be different. In addition, the effect of carbachol on Cl^- secretion is transient (Vajanaphanich et al., 1995; Barrett, 2008), whereas that of Epac is sustained. Carbachol elevates $[Ca^{2+}]_i$ by 350–450 nM (Vajanaphanich et al., 1995), whereas the effect of Epac on $[Ca^{2+}]_i$ is 50 nM (Fig. 5 B). This moderate elevation of $[Ca^{2+}]_i$ and its source from a pool probably distinct from that sensitive to carbachol either does not or is insufficient to fully activate Ca-dependent basolateral K^+ channels, which might provide additional driving force for Cl^- to exit across the apical membrane. Therefore, carbachol exerts a synergistic effect with cAMP on Cl^- secretion, whereas the Epac effect is additive to Sp-8-pCPT-cAMP. In fact, the basolateral membrane also limits the effect of Epac alone on Cl^- secretion. In intact cells, the Epac agonist only had a modest effect. When the basolateral membrane was permeabilized, the Epac agonist had a more enhanced effect on apical Cl^- conductance, which was ~40–50% of that produced by FSK (compare Fig. 6, A with B). This means that fully half of the FSK-stimulated Cl^- conductance at the apical membrane was not due to CFTR. A working model of FSK stimulation of Cl^- secretion in T84 cells is depicted in Fig. 11. This model demonstrates that activation of adenylate cyclase by FSK results in formation of cAMP. Because the effect of FSK could be reproduced by 8-Br-cAMP and by VIP, and the effect of Epac was PKA independent, these findings suggest that PKA and Epac1 are independent downstream effectors of cAMP. Epac1 activates Rap2, which then leads to an increase in $[Ca^{2+}]_i$. PLC ϵ is activated by small GTPases, such as Ras and Rho (Schmidt et al., 2001), and the involvement of PLC was indicated by the elevation of $[Ca^{2+}]_i$ by FSK, which was completely blunted by U73122, and that FSK-stimulated Cl^- secretion was partially blunted by U73122. Because FSK-stimulated Cl^- secretion was inhibited by Gö6976, which selectively inhibits the Ca^{2+} -sensitive conventional PKC isoforms PKC α , PKC β , and PKC γ , candidate PKC isoforms are involved in secretion (Doolen and Zahniser, 2002). We conclude from all of this that the final outcome of Epac activation is a Cl^- secretion through a yet-to-be identified

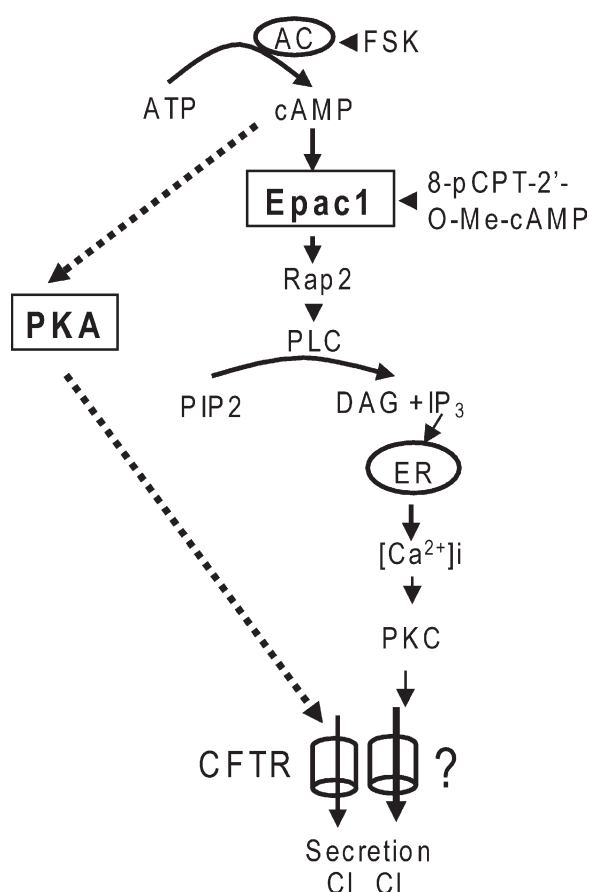


Figure 11. Model showing the FSK-stimulated PKA- and Epac-dependent (PKA-independent) signaling pathways of epithelial Cl^- secretion in T84 cells. The dotted arrows and the solid arrows are used to indicate the PKA or Epac1 pathways, respectively, which run in parallel downstream of cAMP. AC, adenylate cyclase; PLC, phospholipase C; DAG, diacylglycerol; PIP2, phosphatidylinositol 4,5-bisphosphate; IP₃, inositol 1,4,5 triphosphate; ER, endoplasmic reticulum; ?, unknown Cl^- channels regulated by Epac.

channel. This pathway of enhanced Cl^- secretion, independent of the CFTR channel, might be useful in treating cystic fibrosis where the CFTR channel is defective. Thus, Epac1 transduces cAMP signaling into Ca^{2+} signaling, providing an additional pathway to manifest the effects of cAMP on intestinal Cl^- secretion.

To compare the Epac-stimulated Cl^- current to previously identified intestinal epithelial channels, we characterized its ion selectivity, I-V characteristics, and blocker sensitivity. The Epac-mediated current was inwardly rectifying, was sensitive to BAPTA-AM and thus Ca^{2+} sensitive, had a halide selectivity of $\text{Cl}^- > \text{Br}^- > \text{I}^-$, and was not sensitive to Cd^{2+} , Zn^{2+} , CFTRinh-172, or niflumic acid, but was sensitive to DIDS, NPPB, and GlyH-101. CFTR Cl^- currents are distinguished by a linear I-V relation, lack of a time-dependent current decay, activation by PKA, and inhibition by diphenylamine-2-carboxylate, glibenclamide, and CFTRinh-172, but not by DIDS (Gray et al., 1993; McCarty et al., 1993). The halide selectivity sequence most

commonly reported for CFTR is $\text{Br}^- > \text{Cl}^- > \text{I}^-$ (Riordan, 1993). CFTR channels also have a single-channel conductance of 4–10 pS (Fuller and Benos, 2000). In our study, when CHO cells that have endogenous Epac expression (Lorenowicz et al., 2006) were transiently transfected with a plasmid containing human CFTR, 8-pCPT-2'-O-Me-cAMP did not increase the current amplitude, whereas subsequent application of a CFTR-stimulating cocktail of 100 μM cpt-cAMP plus 10 μM FSK activated large, linear currents (Fig. S3). The cpt-cAMP/FSK-activated currents were inhibited by the application of 10 μM CFTRinh-172, demonstrating that the Cl^- conductance stimulated by cpt-cAMP/FSK was a CFTR-mediated conductance. Therefore, it appears that in cells containing CFTR, but not the complete complement of endogenous Cl^- channels found in intestinal epithelial cells, 8-pCPT-2'-O-Me-cAMP fails to activate a Cl^- conductance, strongly supporting our hypothesis that Epac1 does not activate CFTR but another yet unidentified Cl^- channel. The involvement of a non-CFTR Cl^- channel was strongly indicated by the observation that a specific CFTR channel blocker, CFTRinh-172, partially inhibited the cAMP-stimulated Cl^- secretion but was not able to inhibit 8-pCPT-2'-O-Me-cAMP-stimulated apical Cl^- conductance in T84 cells, and that 8-pCPT-2'-O-Me-cAMP itself was unable to activate a CFTR current.

In the past, there were conflicting results about the presence of apical Ca^{2+} -activated Cl^- channels in T84 cells. When nystatin was used to permeabilize basolateral membranes of T84 cells, there was no evidence of Ca^{2+} -stimulated I_{Cl} s (Anderson and Welsh, 1991; Reenstra, 1993). However, other studies showed that carbachol or thapsigargin increased a Cl^- conductance in T84 cells (Barrett et al., 1998; Merlin et al., 1998). The presence of apical Ca^{2+} -sensitive Cl^- conductances in T84 cells was further supported by whole cell patch clamp studies in which Cliff and Frizzell (1990) showed cAMP- and Ca^{2+} -stimulated different Cl^- conductances. Merlin et al. (1998) showed similar results that cAMP increased at least two current components, one of which has features in common with that elicited by Ca^{2+} -elevating agents. Ca^{2+} -activated Cl^- channels generally display $\text{I}^- > \text{Br}^- > \text{Cl}^-$ permeability sequence (Evans and Marty, 1986). The molecular identity of the proteins underlying the ubiquitously expressed Ca^{2+} -dependent anion conductance has remained elusive. CaCC conductances are generally inhibited by DIDS and niflumic acid but have varying responses to NPPB. These channels are also diverse in their biophysical properties, for example, with single-channel conductances ranging from 1 to 70 pS and rectification ranging from strong outward to relatively linear I-V relationships (Marty et al., 1984; Klöckner, 1993). On the other hand, the ubiquitously expressed $\text{ClC}2$, also found to mediate Cl^- secretion in many epithelia, including Caco-2 and T84 monolayers (Gyömörey et al.,

2000; Mohammad-Panah et al., 2001; Cuppoletti et al., 2004), has a single-channel conductance of $\sim 2\text{--}3$ pS (Jordt and Jentsch, 1997; Gyömörey et al., 2000). Finally, ClC-2 has a $\text{Cl}^- > \text{I}^-$ selectivity and is inhibited by Zn^{2+} and Cd^{2+} (Schwiebert et al., 1998; Jentsch et al., 1999).

Our data show that Epac1 signaling stimulates an inwardly rectifying current that is not blocked by Cd^{2+} , Zn^{2+} , niflumic acid, CFTRinh-172, or glibenclamide when the current is directly stimulated by 8-pCPT-2'-O-Me-cAMP. Cl^- currents are completely inhibited by DIDS or NPPB (also blockers of CaCC) when FSK in the presence of CFTRinh-172 is used as stimulus. The FSK-stimulated current is completely blocked by GlyH-101. Although GlyH-101 was a drug often considered as CFTR selective, it also blocks ANO1 (a recently cloned CaCC channel) with high potency (Hartzell et al., 2009). Based on the criteria of rectification and blocker sensitivity, we conclude that the Epac-stimulated channel is not the recently identified CaCC, now called ANO1 (TMEM16A) (Yang et al., 2008). The characteristics of the Epac-mediated Cl^- current of T84 cells do not neatly fit the characteristics of any known epithelial Cl^- channel. There was reasonable evidence in our study to indicate that FSK- and 8-pCPT-2'-O-Me-cAMP-increased $[\text{Ca}^{2+}]_i$ in T84 cells was required for some of the actions of cAMP, "the Epac1- Ca^{2+} pathway" in the activation of Cl^- conductances. It is possible this new conductance is another undocumented calcium-activated I_{Cl} .

In summary, this study identifies an additional cAMP signaling pathway that activates a PKA-independent, Epac-mediated intestinal Cl^- secretion in T84 cells and net ion transport in mouse ileum. The I_{Cl} activated by Epac that we have identified and given an initial biophysical characterization might be useful in cystic fibrosis disease by providing an alternative source of chloride movement when the CFTR channel is defective.

We thank Dr. Mark Donowitz for critical reading of the manuscript.

This work was supported by the Johns Hopkins Center for Global Health (grant 80019485 to C.-M. Tse) and the National Institutes of Health/NIDDK Hopkins Digestive Disease Basic Research Development (grant R24DK064399; mouse core to S.E. Guggino and C.-M. Tse). The Cystic Fibrosis Foundation supported S.E. Guggino (grant R025-CR07).

Angus C. Nairn served as editor.

Submitted: 8 October 2009

Accepted: 8 December 2009

REFERENCES

Anderson, M.P., and M.J. Welsh. 1991. Calcium and cAMP activate different chloride channels in the apical membrane of normal and cystic fibrosis epithelia. *Proc. Natl. Acad. Sci. USA*. 88:6003–6007. doi:10.1073/pnas.88.14.6003

Barrett, K.E. 2000. New insights into the pathogenesis of intestinal dysfunction: secretory diarrhea and cystic fibrosis. *World J. Gastroenterol.* 6:470–474.

Barrett, K.E. 2008. New ways of thinking about (and teaching about) intestinal epithelial function. *Adv. Physiol. Educ.* 32:25–34. doi:10.1152/advan.00092.2007

Barrett, K.E., and S.J. Keely. 2000. Chloride secretion by the intestinal epithelium: molecular basis and regulatory aspects. *Annu. Rev. Physiol.* 62:535–572. doi:10.1146/annurev.physiol.62.1.535

Barrett, K.E., J. Smitham, A. Traynor-Kaplan, and J.M. Uribe. 1998. Inhibition of $\text{Ca}(2+)$ -dependent Cl^- secretion in T84 cells: membrane target(s) of inhibition is agonist specific. *Am. J. Physiol.* 274:C958–C965.

Bos, J.L. 2006. Epac proteins: multi-purpose cAMP targets. *Trends Biochem. Sci.* 31:680–686. doi:10.1016/j.tibs.2006.10.002

Boucher, R.C. 2007. Cystic fibrosis: a disease of vulnerability to airway surface dehydration. *Trends Mol. Med.* 13:231–240. doi:10.1016/j.molmed.2007.05.001

Cass, A., A. Finkelstein, and V. Krespi. 1970. The ion permeability induced in thin lipid membranes by the polyene antibiotics nystatin and amphotericin B. *J. Gen. Physiol.* 56:100–124. doi:10.1085/jgp.56.1.100

Chijiwa, T., A. Mishima, M. Hagiwara, M. Sano, K. Hayashi, T. Inoue, K. Naito, T. Toshioka, and H. Hidaka. 1990. Inhibition of forskolin-induced neurite outgrowth and protein phosphorylation by a newly synthesized selective inhibitor of cyclic AMP-dependent protein kinase, N-[2-(p-bromocinnamylamino)ethyl]-5-isoquinolinesulfonamide (H-89), of PC12D pheochromocytoma cells. *J. Biol. Chem.* 265:5267–5272.

Christensen, A.E., F. Selheim, J. de Rooij, S. Dremier, F. Schwede, K.K. Dao, A. Martinez, C. Maenhaut, J.L. Bos, H.G. Genieser, and S.O. Døskeland. 2003. cAMP analog mapping of Epac1 and cAMP kinase. Discriminating analogs demonstrate that Epac and cAMP kinase act synergistically to promote PC-12 cell neurite extension. *J. Biol. Chem.* 278:35394–35402. doi:10.1074/jbc.M302179200

Cliff, W.H., and R.A. Frizzell. 1990. Separate Cl^- conductances activated by cAMP and Ca^{2+} in Cl^- -secreting epithelial cells. *Proc. Natl. Acad. Sci. USA*. 87:4956–4960. doi:10.1073/pnas.87.13.4956

Conway, B.E. 1981. Ionic Hydration in Chemistry and Biophysics (Studies in Physical and Theoretical Chemistry). Elsevier, New York. 804 pp.

Cuppoletti, J., D.H. Malinowska, K.P. Tewari, Q.J. Li, A.M. Sherry, M.L. Patchen, and R. Ueno. 2004. SPI-0211 activates T84 cell chloride transport and recombinant human ClC-2 chloride currents. *Am. J. Physiol. Cell Physiol.* 287:C1173–C1183. doi:10.1152/ajpcell.00528.2003

Davies, S.P., H. Reddy, M. Caivano, and P. Cohen. 2000. Specificity and mechanism of action of some commonly used protein kinase inhibitors. *Biochem. J.* 351:95–105. doi:10.1042/0264-6021:3510095

de Rooij, J., F.J. Zwartkruis, M.H. Verheijen, R.H. Cool, S.M. Nijman, A. Wittinghofer, and J.L. Bos. 1998. Epac is a Rap1 guanine-nucleotide-exchange factor directly activated by cyclic AMP. *Nature*. 396:474–477. doi:10.1038/24884

Denning, G.M., R.A. Clark, and M.J. Welsh. 1994. cAMP and inositol 1,4,5-trisphosphate increase Ca^{2+} in HT-29 cells by activating different Ca^{2+} influx pathways. *Am. J. Physiol.* 267:C776–C783.

Dharmasathaphorn, K., and J.L. Madara. 1990. Established intestinal cell lines as model systems for electrolyte transport studies. *Methods Enzymol.* 192:354–389. doi:10.1016/0076-6879(90)92082-O

Doolen, S., and N.R. Zahniser. 2002. Conventional protein kinase C isoforms regulate human dopamine transporter activity in *Xenopus* oocytes. *FEBS Lett.* 516:187–190. doi:10.1016/S0014-5793(02)02554-1

Dyachok, O., and E. Gylfe. 2004. $\text{Ca}(2+)$ -induced $\text{Ca}(2+)$ release via inositol 1,4,5-trisphosphate receptors is amplified by protein kinase A and triggers exocytosis in pancreatic beta-cells. *J. Biol. Chem.* 279:45455–45461. doi:10.1074/jbc.M407673200

- Dyachok, O., G. Tufveson, and E. Gylfe. 2004. Ca²⁺-induced Ca²⁺ release by activation of inositol 1,4,5-trisphosphate receptors in primary pancreatic beta-cells. *Cell Calcium*. 36:1–9. doi:10.1016/j.ceca.2003.11.004
- Evans, M.G., and A. Marty. 1986. Calcium-dependent chloride currents in isolated cells from rat lacrimal glands. *J. Physiol.* 378:437–460.
- Evellin, S., J. Nolte, K. Tysack, F. vom Dorp, M. Thiel, P.A. Weernink, K.H. Jakobs, E.J. Webb, J.W. Lomasney, and M. Schmidt. 2002. Stimulation of phospholipase C-epsilon by the M3 muscarinic acetylcholine receptor mediated by cyclic AMP and the GTPase Rap2B. *J. Biol. Chem.* 277:16805–16813. doi:10.1074/jbc.M112024200
- Factor, P., G.M. Mutlu, L. Chen, J. Mohameed, A.T. Akhmedov, F.J. Meng, T. Jilling, E.R. Lewis, M.D. Johnson, A. Xu, et al. 2007. Adenosine regulation of alveolar fluid clearance. *Proc. Natl. Acad. Sci. USA*. 104:4083–4088. doi:10.1073/pnas.0601117104
- Fuller, C.M., and D.J. Benos. 2000. Ca(2+)-activated Cl(-) channels: a newly emerging anion transport family. *News Physiol. Sci.* 15:165–171.
- Gray, M.A., S. Plant, and B.E. Argent. 1993. cAMP-regulated whole cell chloride currents in pancreatic duct cells. *Am. J. Physiol.* 264:C591–C602.
- Gyömörey, K., H. Yeger, C. Ackerley, E. Garami, and C.E. Bear. 2000. Expression of the chloride channel ClC-2 in the murine small intestine epithelium. *Am. J. Physiol. Cell Physiol.* 279:C1787–C1794.
- Hartzell, C., I. Putzier, and J. Arreola. 2005. Calcium-activated chloride channels. *Annu. Rev. Physiol.* 67:719–758. doi:10.1146/annurev.physiol.67.032003.154341
- Hartzell, H.C., K. Yu, Q. Xiao, L.T. Chien, and Z. Qu. 2009. Anoctamin/TMEM16 family members are Ca²⁺-activated Cl⁻ channels. *J. Physiol.* 587:2127–2139. doi:10.1113/jphysiol.2008.163709
- Hidaka, H., and R. Kobayashi. 1992. Pharmacology of protein kinase inhibitors. *Annu. Rev. Pharmacol. Toxicol.* 32:377–397. doi:10.1146/annurev.pa.32.040192.002113
- Hidaka, H., M. Hagiwara, and T. Chijiwa. 1990. Molecular pharmacology of protein kinases. *Neurochem. Res.* 15:431–434. doi:10.1007/BF00969929
- Hillesheim, J., B. Riederer, B. Tuo, M. Chen, M. Manns, J. Biber, C. Yun, O. Kocher, and U. Seidler. 2007. Down regulation of small intestinal ion transport in PDZK1- (CAP70/NHERF3) deficient mice. *Pflugers Arch.* 454:575–586. doi:10.1007/s00424-007-0239-x
- Holz, G.G. 2004. Epac: A new cAMP-binding protein in support of glucagon-like peptide-1 receptor-mediated signal transduction in the pancreatic beta-cell. *Diabetes*. 53:5–13. doi:10.2337/diabetes.53.1.5
- Hoque, K.M., V.M. Rajendran, and H.J. Binder. 2005. Zinc inhibits cAMP-stimulated Cl secretion via basolateral K-channel blockade in rat ileum. *Am. J. Physiol. Gastrointest. Liver Physiol.* 288:G956–G963. doi:10.1152/ajpgi.00441.2004
- Huang, P., K. Trotter, R.C. Boucher, S.L. Milgram, and M.J. Stutts. 2000. PKA holoenzyme is functionally coupled to CFTR by AKAPs. *Am. J. Physiol. Cell Physiol.* 278:C417–C422.
- Huflejt, M.E., R.A. Blum, S.G. Miller, H.P.H. Moore, and T.E. Machen. 1994. Regulated Cl transport, K and Cl permeability, and exocytosis in T84 cells. *J. Clin. Invest.* 93:1900–1910. doi:10.1172/JCI117181
- Jentsch, T.J., T. Friedrich, A. Schriever, and H. Yamada. 1999. The ClC chloride channel family. *Pflugers Arch.* 437:783–795. doi:10.1007/s004240050847
- Jordt, S.E., and T.J. Jentsch. 1997. Molecular dissection of gating in the ClC-2 chloride channel. *EMBO J.* 16:1582–1592. doi:10.1093/emboj/16.7.1582
- Kang, G., J.W. Joseph, O.G. Chepurny, M. Monaco, M.B. Wheeler, J.L. Bos, F. Schwede, H.G. Genieser, and G.G. Holz. 2003. Epac-selective cAMP analog 8-pCPT-2'-O-Me-cAMP as a stimulus for Ca²⁺-induced Ca²⁺ release and exocytosis in pancreatic beta-cells. *J. Biol. Chem.* 278:8279–8285. doi:10.1074/jbc.M211682200
- Kang, G., C.A. Leech, O.G. Chepurny, W.A. Coetzee, and G.G. Holz. 2008. Role of the cAMP sensor Epac as a determinant of KATP channel ATP sensitivity in human pancreatic beta-cells and rat INS-1 cells. *J. Physiol.* 586:1307–1319. doi:10.1113/jphysiol.2007.143818
- Kawasaki, H., G.M. Springett, N. Mochizuki, S. Toki, M. Nakaya, M. Matsuda, D.E. Housman, and A.M. Graybiel. 1998. A family of cAMP-binding proteins that directly activate Rap1. *Science*. 282:2275–2279. doi:10.1126/science.282.5397.2275
- Kidd, J.F., and P. Thorn. 2000. Intracellular Ca²⁺ and Cl⁻ channel activation in secretory cells. *Annu. Rev. Physiol.* 62:493–513. doi:10.1146/annurev.physiol.62.1.493
- Kleppisch, T., and M.T. Nelson. 1995. Adenosine activates ATP-sensitive potassium channels in arterial myocytes via A2 receptors and cAMP-dependent protein kinase. *Proc. Natl. Acad. Sci. USA*. 92:12441–12445. doi:10.1073/pnas.92.26.12441
- Klöckner, U. 1993. Intracellular calcium ions activate a low-conductance chloride channel in smooth-muscle cells isolated from human mesenteric artery. *Pflugers Arch.* 424:231–237. doi:10.1007/BF00384347
- Lewis, S.A., D.C. Eaton, C. Clausen, and J.M. Diamond. 1977. Nystatin as a probe for investigating the electrical properties of a tight epithelium. *J. Gen. Physiol.* 70:427–440. doi:10.1085/jgp.70.4.427
- Lochner, A., and J.A. Moolman. 2006. The many faces of H89: a review. *Cardiovasc. Drug Rev.* 24:261–274. doi:10.1111/j.1527-3466.2006.00261.x
- Lorenowicz, M.J., J. van Gils, M. de Boer, P.L. Hordijk, and M. Fernandez-Borja. 2006. Epac1-Rap1 signaling regulates monocyte adhesion and chemotaxis. *J. Leukoc. Biol.* 80:1542–1552. doi:10.1189/jlb.0506357
- Ma, T., J.R. Thiagarajah, H. Yang, N.D. Sonawane, C. Folli, L.J. Galletta, and A.S. Verkman. 2002. Thiazolidinone CFTR inhibitor identified by high-throughput screening blocks cholera toxin-induced intestinal fluid secretion. *J. Clin. Invest.* 110:1651–1658.
- Maly, K., G. Hechenberger, K. Strese, I. Tinhofer, I. Wede, W. Doppler, and H.H. Grunicke. 2007. Regulation of calcium signalling by the small GTP-binding proteins Ras and Rac1. *Adv. Enzyme Regul.* 47:169–183. doi:10.1016/j.advenzreg.2006.12.017
- Marty, A., Y.P. Tan, and A. Trautmann. 1984. Three types of calcium-dependent channel in rat lacrimal glands. *J. Physiol.* 357:293–325.
- McCarthy, N.A., S. McDonough, B.N. Cohen, J.R. Riordan, N. Davidson, and H.A. Lester. 1993. Voltage-dependent block of the cystic fibrosis transmembrane conductance regulator Cl⁻ channel by two closely related arylaminobenzoates. *J. Gen. Physiol.* 102:1–23. doi:10.1085/jgp.102.1.1
- Merlin, D., L. Jiang, G.R. Strohmeier, A. Nusrat, S.L. Alper, W.I. Lencer, and J.L. Madara. 1998. Distinct Ca²⁺ and cAMP-dependent anion conductances in the apical membrane of polarized T84 cells. *Am. J. Physiol.* 275:C484–C495.
- Mohammad-Panah, R., K. Gyomory, J. Rommens, M. Choudhury, C. Li, Y. Wang, and C.E. Bear. 2001. ClC-2 contributes to native chloride secretion by a human intestinal cell line, Caco-2. *J. Biol. Chem.* 276:8306–8313. doi:10.1074/jbc.M006764200
- Mun, E.C., J.M. Mayol, M. Riegler, T.C. O'Brien, O.C. Farokhzad, J.C. Song, C. Pothoulakis, B.J. Hrnjez, and J.B. Matthews. 1998. Levamisole inhibits intestinal Cl⁻ secretion via basolateral K⁺ channel blockade. *Gastroenterology*. 114:1257–1267. doi:10.1016/S0016-5085(98)70432-9
- Muroi, M., and T. Suzuki. 1993. Role of protein kinase A in LPS-induced activation of NF-kappa B proteins of a mouse macrophage-like cell line, J774. *Cell. Signal.* 5:289–298. doi:10.1016/0898-6568(93)90019-I

- Pereira, L., M. Métrich, M. Fernández-Velasco, A. Lucas, J. Leroy, R. Perrier, E. Morel, R. Fischmeister, S. Richard, J.P. Bénitah, et al. 2007. The cAMP binding protein Epac modulates Ca²⁺ sparks by a Ca²⁺/calmodulin kinase signalling pathway in rat cardiac myocytes. *J. Physiol.* 583:685–694. doi:10.1113/jphysiol.2007.133066
- Reenstra, W.W. 1993. Inhibition of cAMP- and Ca-dependent Cl-secretion by phorbol esters: inhibition of basolateral K⁺ channels. *Am. J. Physiol.* 264:C161–C168.
- Riordan, J.R. 1993. The cystic fibrosis transmembrane conductance regulator. *Annu. Rev. Physiol.* 55:609–630. doi:10.1146/annurev.ph.55.030193.003141
- Schmidt, M., S. Evellin, P.A. Weernink, F. von Dorp, H. Rehmann, J.W. Lomasney, and K.H. Jakobs. 2001. A new phospholipase-C-calcium signalling pathway mediated by cyclic AMP and a Rap GTPase. *Nat. Cell Biol.* 3:1020–1024. doi:10.1038/ncb1101-1020
- Schultz, B.D., A.D. DeRoos, C.J. Venglarik, A.K. Singh, R.A. Frizzell, and R.J. Bridges. 1996. Glibenclamide blockade of CFTR chloride channels. *Am. J. Physiol.* 271:L192–L200.
- Schwiebert, E.M., L.P. Cid-Soto, D. Stafford, M. Carter, C.J. Blaisdell, P.L. Zeitlin, W.B. Guggino, and G.R. Cutting. 1998. Analysis of ClC-2 channels as an alternative pathway for chloride conduction in cystic fibrosis airway cells. *Proc. Natl. Acad. Sci. USA.* 95:3879–3884. doi:10.1073/pnas.95.7.3879
- Semrad, C.E., and E.B. Chang. 1987. Calcium-mediated cyclic AMP inhibition of Na-H exchange in small intestine. *Am. J. Physiol.* 252:C315–C322.
- Sheppard, D.N., and K.A. Robinson. 1997. Mechanism of glibenclamide inhibition of cystic fibrosis transmembrane conductance regulator Cl[−] channels expressed in a murine cell line. *J. Physiol.* 503:333–346. doi:10.1111/j.1469-7793.1997.333bh.x
- Thelin, W.R., and R.C. Boucher. 2007. The epithelium as a target for therapy in cystic fibrosis. *Curr. Opin. Pharmacol.* 7:290–295. doi:10.1016/j.coph.2007.01.004
- Vajanaphanich, M., C. Schultz, R.Y. Tsien, A.E. Traynor-Kaplan, S.J. Pandol, and K.E. Barrett. 1995. Cross-talk between calcium and cAMP-dependent intracellular signaling pathways. Implications for synergistic secretion in T84 colonic epithelial cells and rat pancreatic acinar cells. *J. Clin. Invest.* 96:386–393. doi:10.1172/JCI118046
- Verkman, A.S., and L.J. Galletta. 2009. Chloride channels as drug targets. *Nat. Rev. Drug Discov.* 8:153–171. doi:10.1038/nrd2780
- Wang, D., Y. Sun, W. Zhang, and P. Huang. 2008. Apical adenosine regulates basolateral Ca²⁺-activated potassium channels in human airway Calu-3 epithelial cells. *Am. J. Physiol. Cell Physiol.* 294:C1443–C1453. doi:10.1152/ajpcell.00556.2007
- Yang, Y.D., H. Cho, J.Y. Koo, M.H. Tak, Y. Cho, W.S. Shim, S.P. Park, J. Lee, B. Lee, B.M. Kim, et al. 2008. TMEM16A confers receptor-activated calcium-dependent chloride conductance. *Nature.* 455:1210–1215. doi:10.1038/nature07313
- Yip, K.P. 2006. Epac-mediated Ca(2+) mobilization and exocytosis in inner medullary collecting duct. *Am. J. Physiol. Renal Physiol.* 291:F882–F890. doi:10.1152/ajprenal.00411.2005